




Experiments on crystal radiators at DESY TB and CERN PS

2nd FCC-France&Italy workshop – Venice 

Nicola Canale

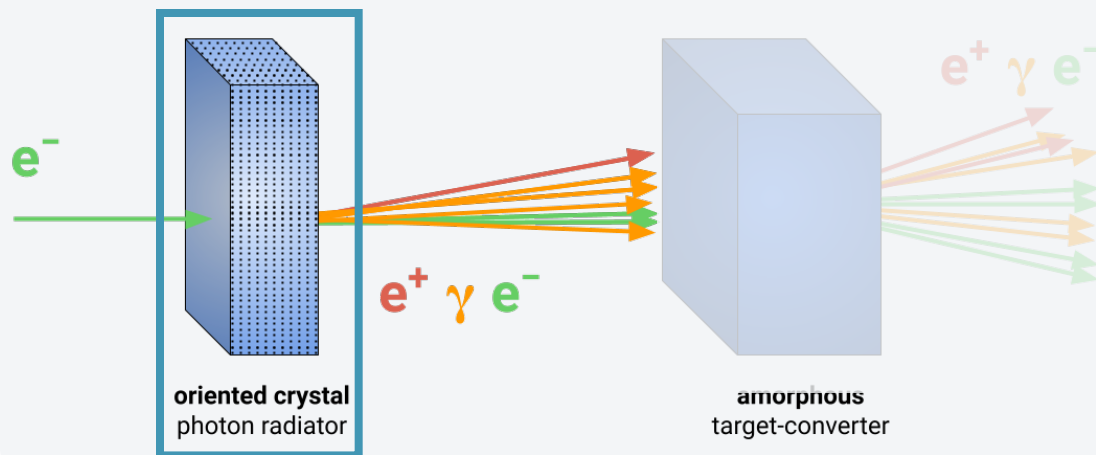
on behalf of F. Alharthi, A. Bacci, L. Bandiera, D. Boccanfuso, S. Carsi, I. Chaikovska, R. Chehab, D. De Salvador, P. Fedeli, V. Guidi, V. Haurylavets, O. Iorio, G. Lezzani, L. Malagutti, S. Mangiacavalli, A. Mazzolari, P. Monti Guarnieri, V. Mytrochenko, R. Negrello, G. Paternò, M. Prest, M. Romagnoni, M. Rossetti Conti, A. Selmi, F. Sgarbossa, M. Soldani, A. Sytov, V. Tikhomirov, E. Vallazza

INFN Ferrara
ncanale@fe.infn.it

Outlook

As presented in talks by A. Sytov and G. Paternò, **crystal-based positron sources** offer promising potential for future colliders.

Here, we will see the **test beam results on crystal radiators** which serve as a crucial **benchmark for simulation code validation**.



Outlook

As presented in talks by **A. Sytov** and **G. Paternò**, **crystal-based positron sources** offer promising potential for future colliders.

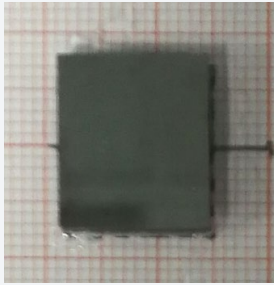
Here, we will see the **test beam results** on **crystal radiators** which serve as a crucial **benchmark** for **simulation code** validation.

- **THE CRYSTALS**
- **EXPERIMENTAL SETUP**
- **TESTBEAM RESULTS**

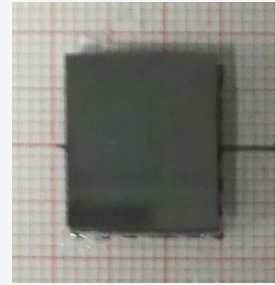
THE CRYSTALS



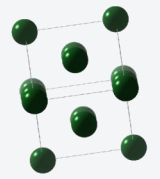
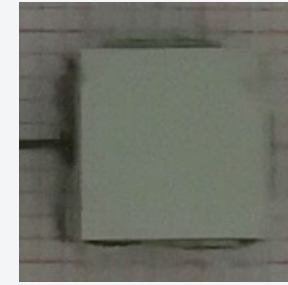
Crystal radiators



Material: **Tungsten (W)**
channelling Axis: **<100>**
 $\theta_C \approx 0.5 \text{ mrad}$
Thickness: **2.25 mm (0.64 X0)**
(**research center** manufactured crystal)



Material: **Tungsten (W)**
channelling Axis: **<111>** (most efficient)
 $\theta_C \approx 0.6 \text{ mrad}$
Thickness: **1.5-2 mm (0.43 – 0.57 X0)**
(**industrially** manufactured crystals)



Material: **Iridium (Ir)**
channelling Axis: **<110>** (most efficient)
 $\theta_C \approx 0.6$
Thickness: **1 -2 mm (0.34 – 0.68 X0)**
(**industrially** manufactured crystals)

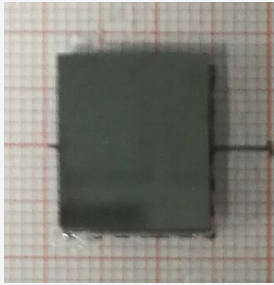
Tested at DESY T21 beamline with 5.6 GeV/c electrons



Tested at CERN PS T9 beamline with 6 GeV/c electrons



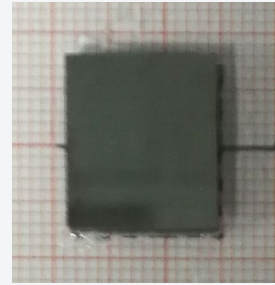
Crystal radiators



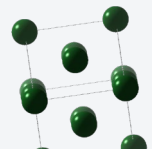
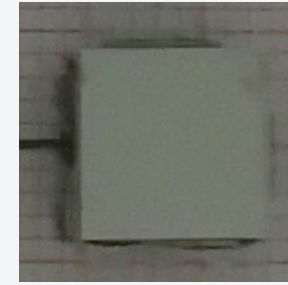
Material: **Tungsten (W)**
channelling Axis: **<100>**
 $\theta_C \approx 0.5 \text{ mrad}$
Thickness: **2.25 mm (0.64 X0)**
(**research center** manufactured crystal)

Research Center quality crystal

Tested at DESY T21 beamline with 5.6 GeV/c electrons



Material: **Tungsten (W)**
channelling Axis: **<111>** (most efficient)
 $\theta_C \approx 0.6 \text{ mrad}$
Thickness: **1.5-2 mm (0.43 – 0.57 X0)**
(**industrially** manufactured crystals)

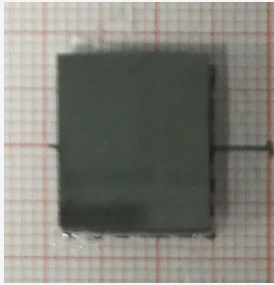


Material: **Iridium (Ir)**
channelling Axis: **<110>** (most efficient)
 $\theta_C \approx 0.6$
Thickness: **1 -2 mm (0.34 – 0.68 X0)**
(**industrially** manufactured crystals)

Tested at CERN PS T9 beamline with 6 GeV/c electrons



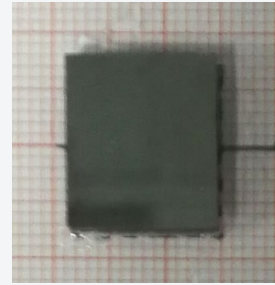
Crystal radiators



Material: **Tungsten (W)**
channelling Axis: **<100>**
 $\theta_C \approx 0.5 \text{ mrad}$
Thickness: **2.25 mm (0.64 X0)**
(**research center** manufactured crystal)

Research Center quality crystal

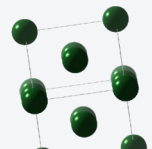
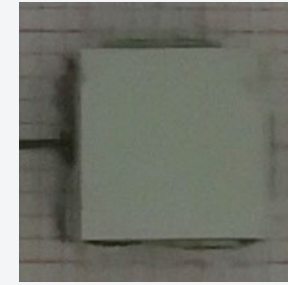
Tested at DESY T21 beamline with 5.6 GeV/c electrons



Material: **Tungsten (W)**
channelling Axis: **<111>** (most efficient)
 $\theta_C \approx 0.6 \text{ mrad}$
Thickness: **1.5-2 mm (0.43 – 0.57 X0)**
(**industrially** manufactured crystals)

W 2mm baseline for Hybrid source radiator - 1.5mm for optimization studies

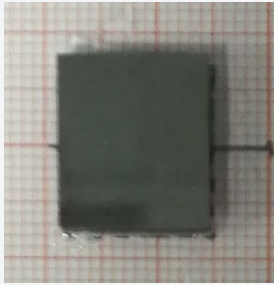
Tested at CERN PS T9 beamline with 6 GeV/c electrons



Material: **Iridium (Ir)**
channelling Axis: **<110>** (most efficient)
 $\theta_C \approx 0.6$
Thickness: **1 -2 mm (0.34 – 0.68 X0)**
(**industrially** manufactured crystals)



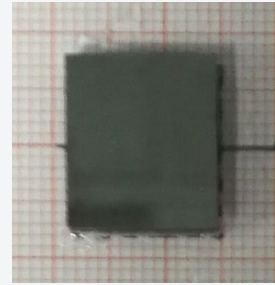
Crystal radiators



Material: **Tungsten (W)**
channelling Axis: **<100>**
 $\theta_C \approx 0.5 \text{ mrad}$
Thickness: **2.25 mm (0.64 X0)**
(**research center** manufactured crystal)

Research Center quality crystal

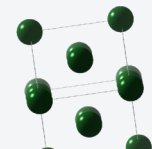
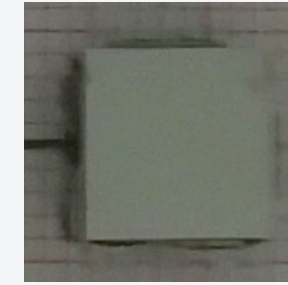
Tested at DESY T21 beamline with 5.6 GeV/c electrons



Material: **Tungsten (W)**
channelling Axis: **<111>** (most efficient)
 $\theta_C \approx 0.6 \text{ mrad}$
Thickness: **1.5-2 mm (0.43 – 0.57 X0)**
(**industrially** manufactured crystals)

W 2mm baseline for Hybrid source radiator - 1.5mm for optimization studies

Tested at CERN PS T9 beamline with 6 GeV/c electrons



Material: **Iridium (Ir)**
channelling Axis: **<110>** (most efficient)
 $\theta_C \approx 0.6$
Thickness: **1 -2 mm (0.34 – 0.68 X0)**
(**industrially** manufactured crystals)

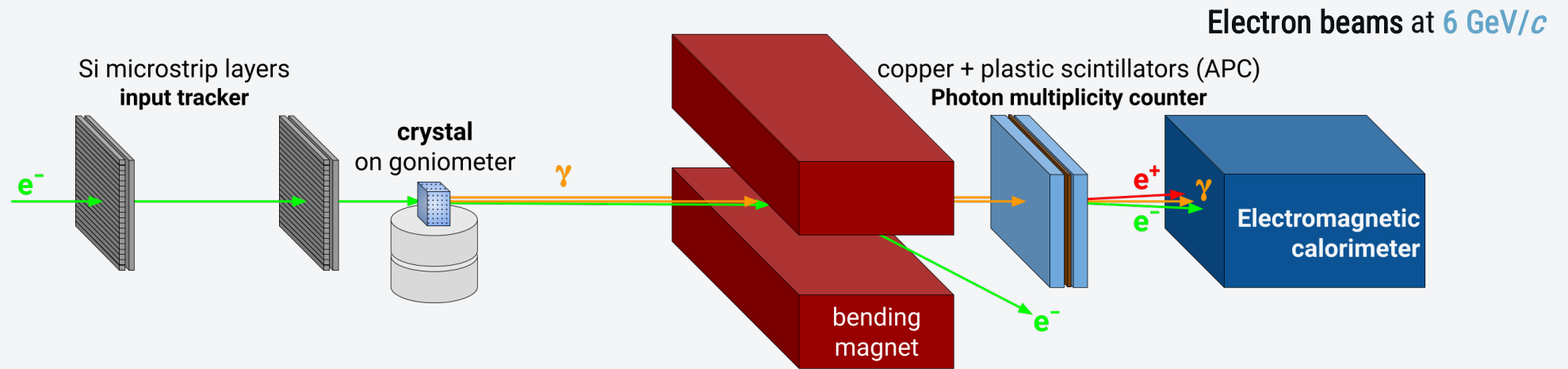
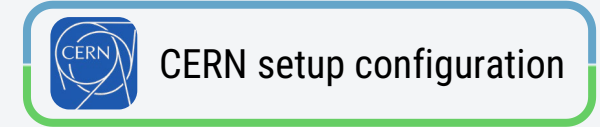
Higher potential, interesting alternative



EXPERIMENTAL SETUP

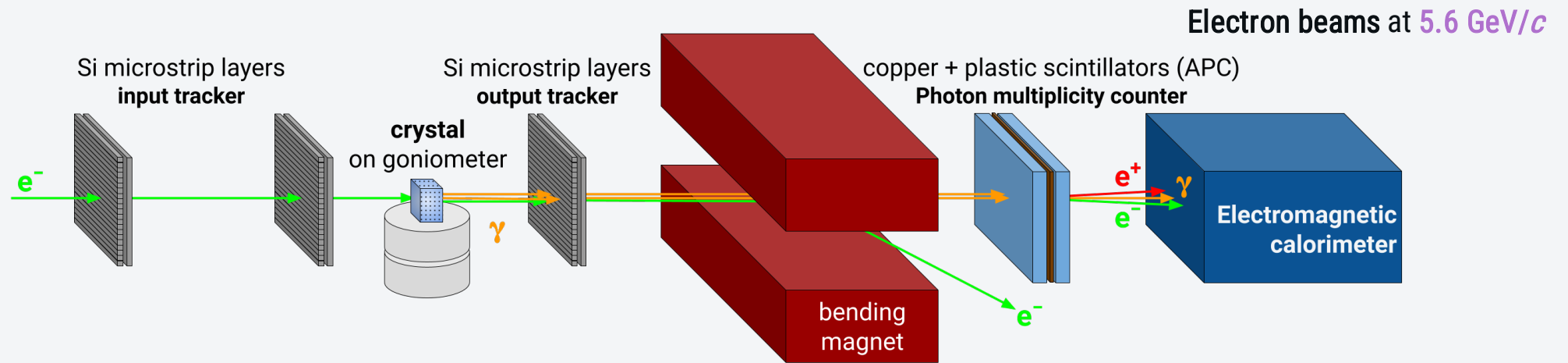


The setup



Provided by INFN Milano Bicocca team – Erik Vallazza & Michela Prest

The setup

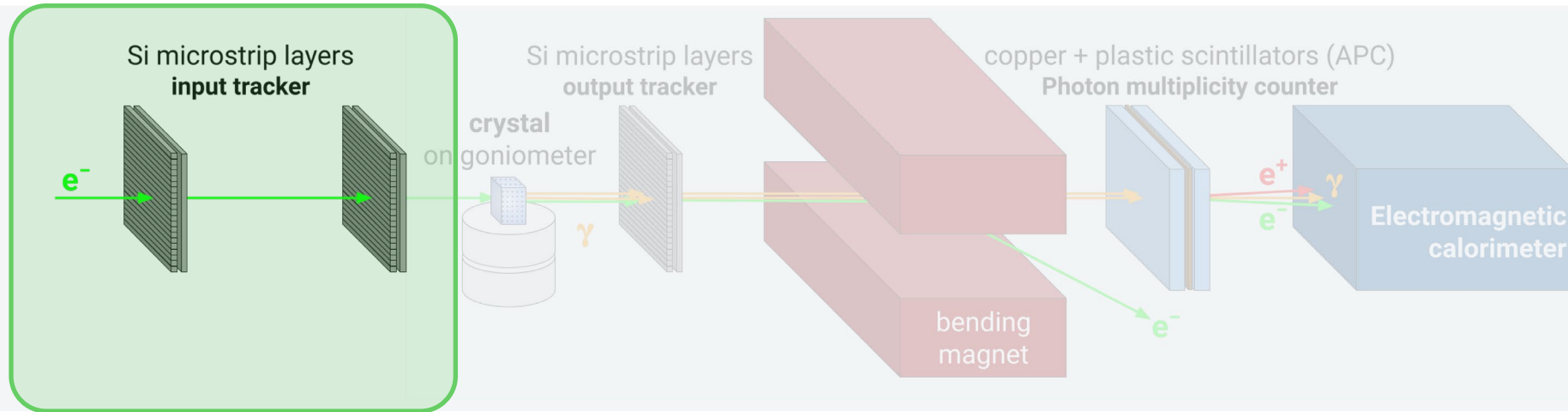


Provided by INFN Milano Bicocca team – Erik Vallazza & Michela Prest

The setup

CERN
configuration

DESY
configuration



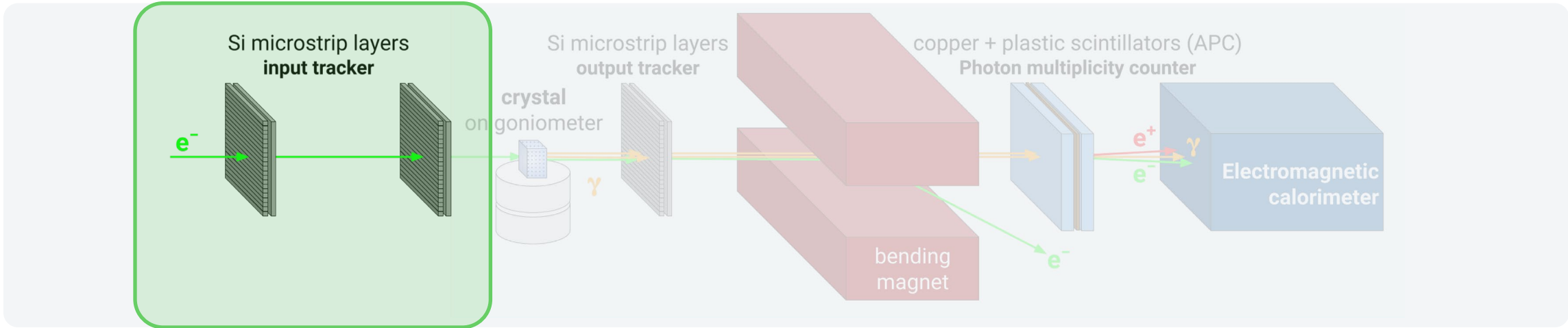
Input stage

Reconstruct track and
impinging angle on the
crystal

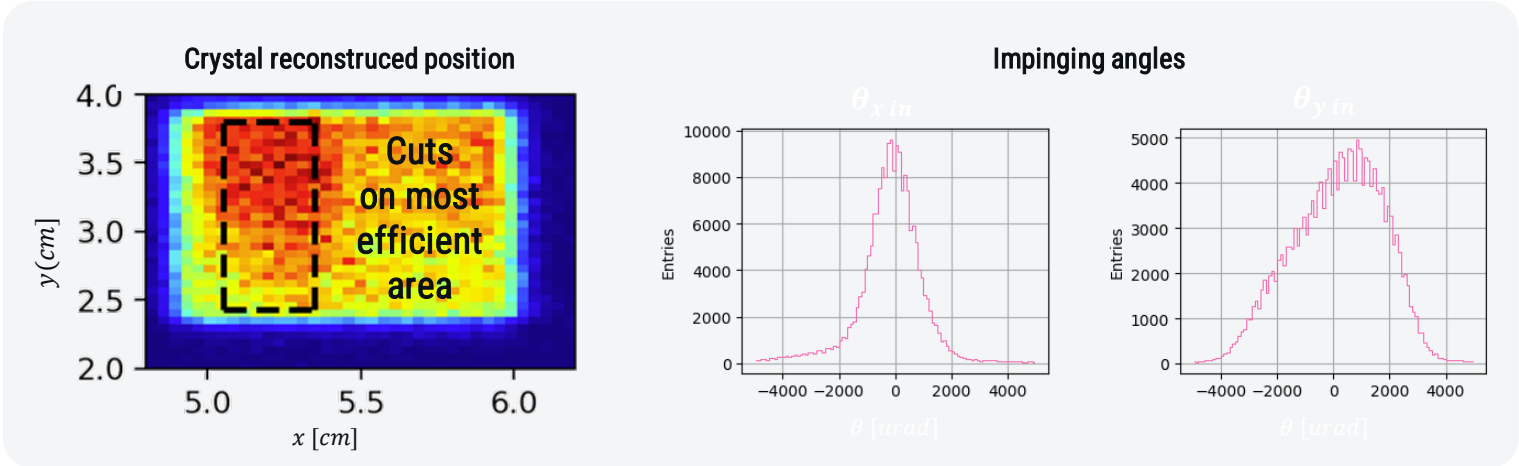
The setup

CERN configuration

DESY configuration



Input stage
Reconstruct track and impinging angle on the crystal



The setup - input stage

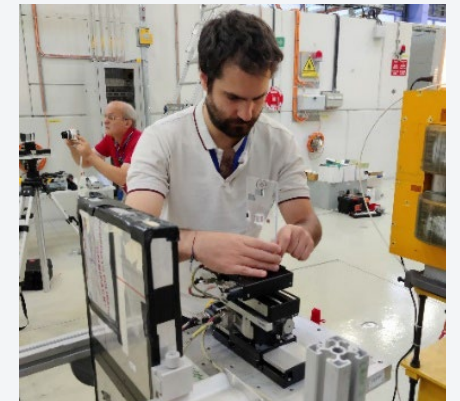
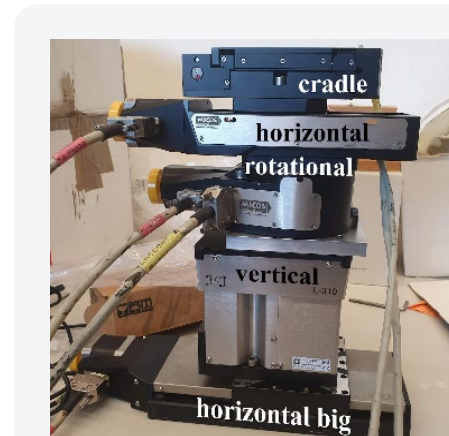
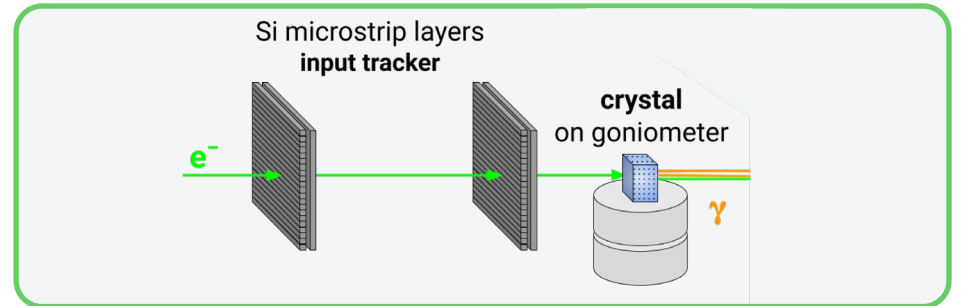
Input tracker

~ $2 \times 2 \text{ cm}^2$ xy double-sided Si microstrip sensors, with an overall $\sim 10 \text{ }\mu\text{m}$ single-hit resolution.

~ $9.5 \times 9.5 \text{ cm}^2$ xy double-sided Si microstrip sensors, with an overall $\sim 40 \text{ }\mu\text{m}$ single-hit resolution.

Goniometer from LNL & UNIPD

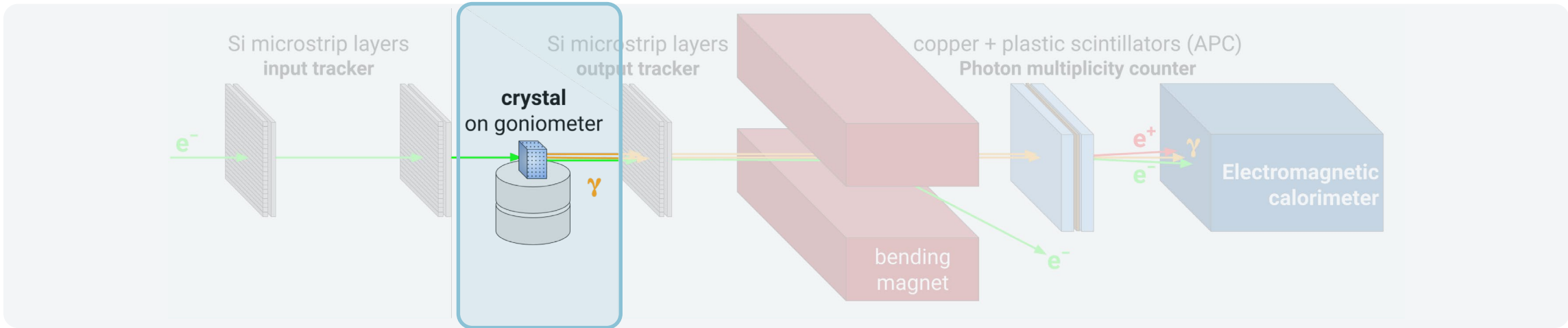
Fine-grained, remote-controlled movements along x, y, θ_x and θ_y with $\sim 5 \text{ }\mu\text{m}$, $1 \text{ }\mu\text{rad}$ resolution.



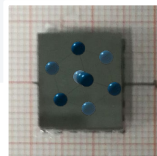
The setup - the crystal

CERN configuration

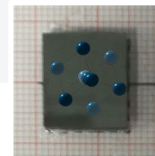
DESY configuration



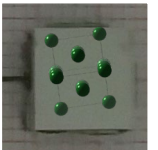
Material: Tungsten (2.25 mm)
channelling Axis: $\langle 100 \rangle$
Axial potential: 1 keV
 $\theta_c \approx 0.5 \text{ mrad}$



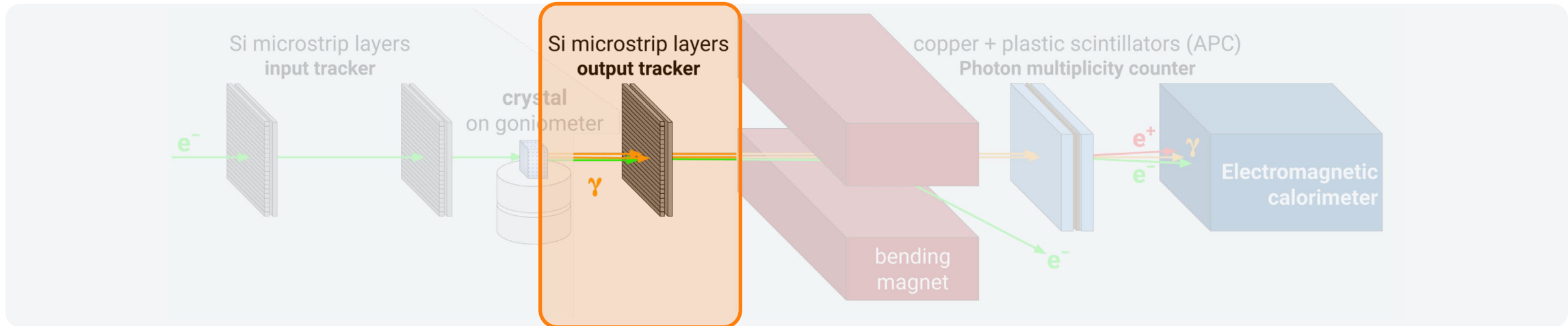
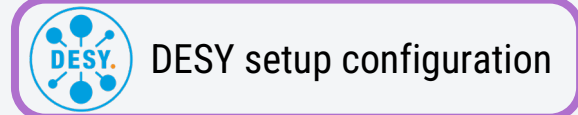
Material: Tungsten (1.5-2 mm)
channelling Axis: $\langle 111 \rangle$
Axial potential: 1 keV
 $\theta_c \approx 0.6 \text{ mrad}$



Material: Iridium (1-2 mm)
channelling Axis: $\langle 110 \rangle$
Axial potential: 1 keV
 $\theta_c \approx 0.6 \text{ mrad}$



The setup - **output tracker**

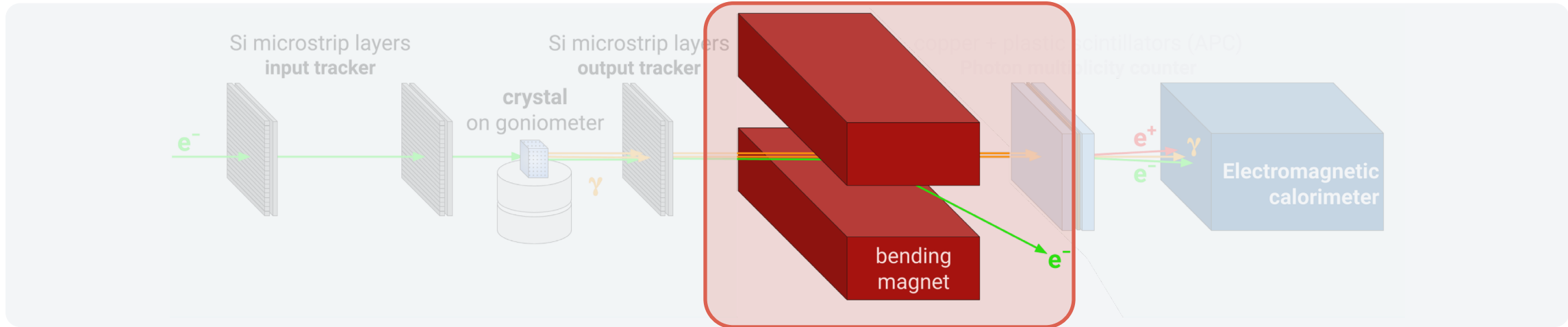


output tracker
As multiplicity counter to align the
crystal

The setup - magnet

CERN
configuration

DESY
configuration

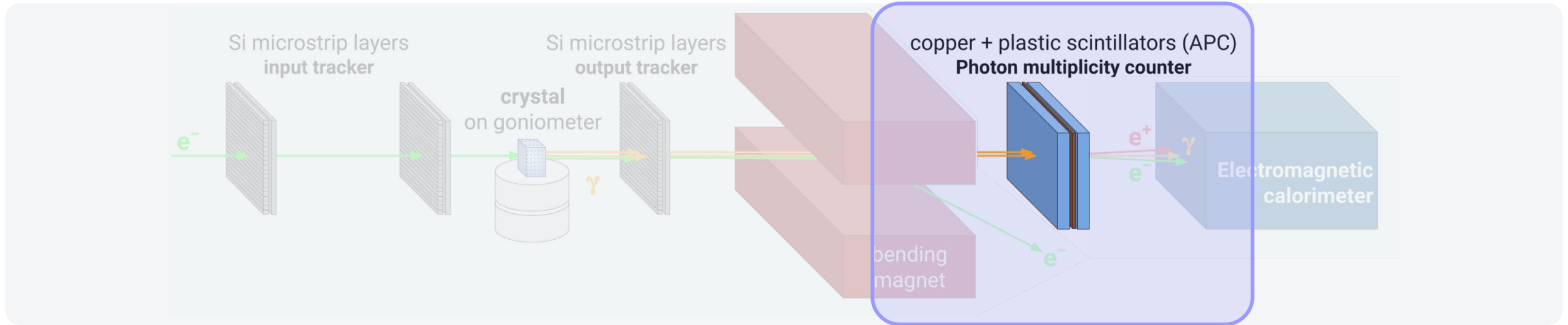


Magnet
Select only the photons

The setup - output stage

CERN
configuration

DESY
configuration

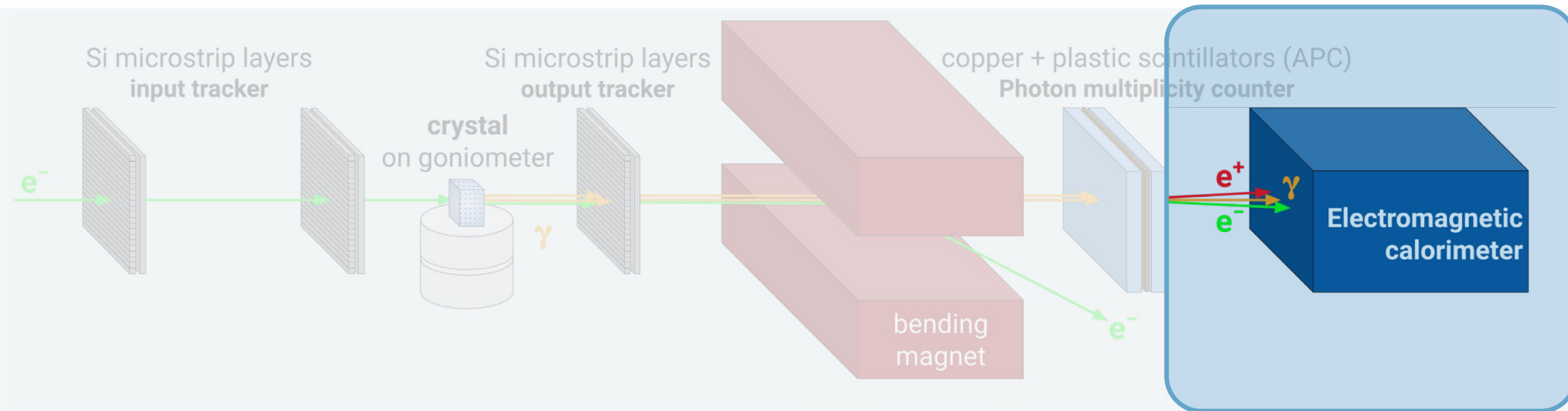


APC + Cu converter
Photon multiplicity counter

The setup - output stage

CERN
configuration

DESY
configuration



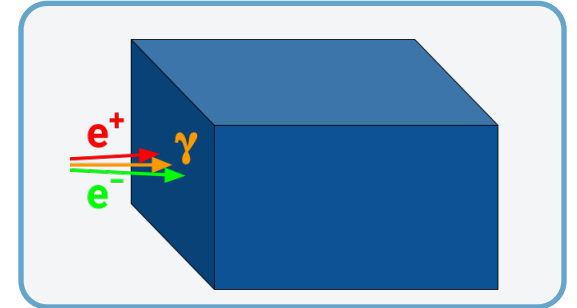
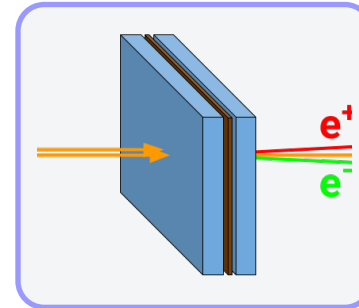
**Radiated energy loss
calorimeter signal**

The setup - output stage

An **Active Photon Converter (APC)** based on plastic scintillators and thin layers of copper ($0.2X_0$) for photo conversion

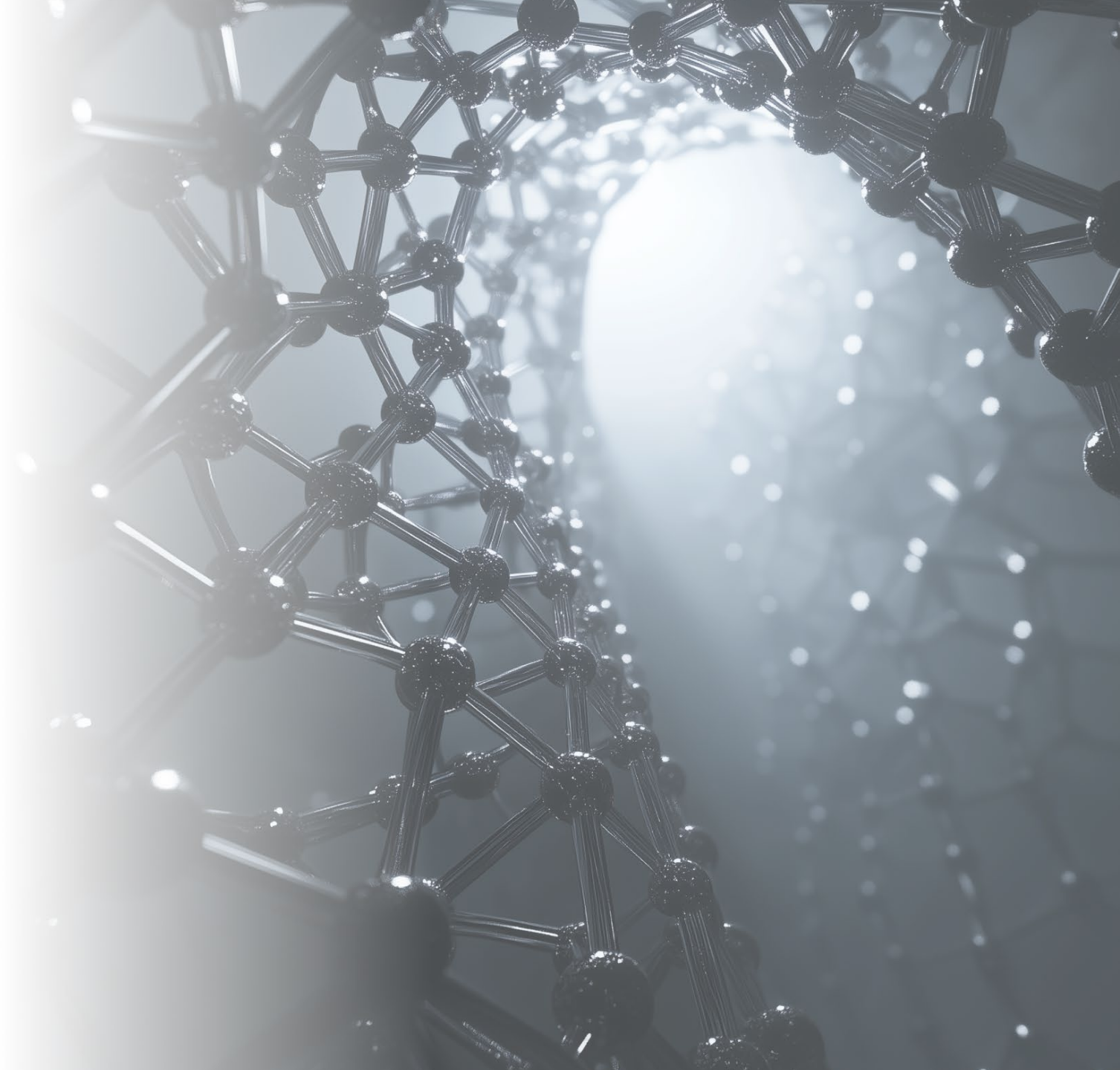
Calorimeters consists in

- 3×3 matrix of **BGO** blocks, PMT-based readout
- (OPAL) **Lead glass blocks** read out by PMTs



Active Photon Converter (APC)

TESTBEAM RESULTS



DESY T21 line

Electron beams at 5.6 GeV/c

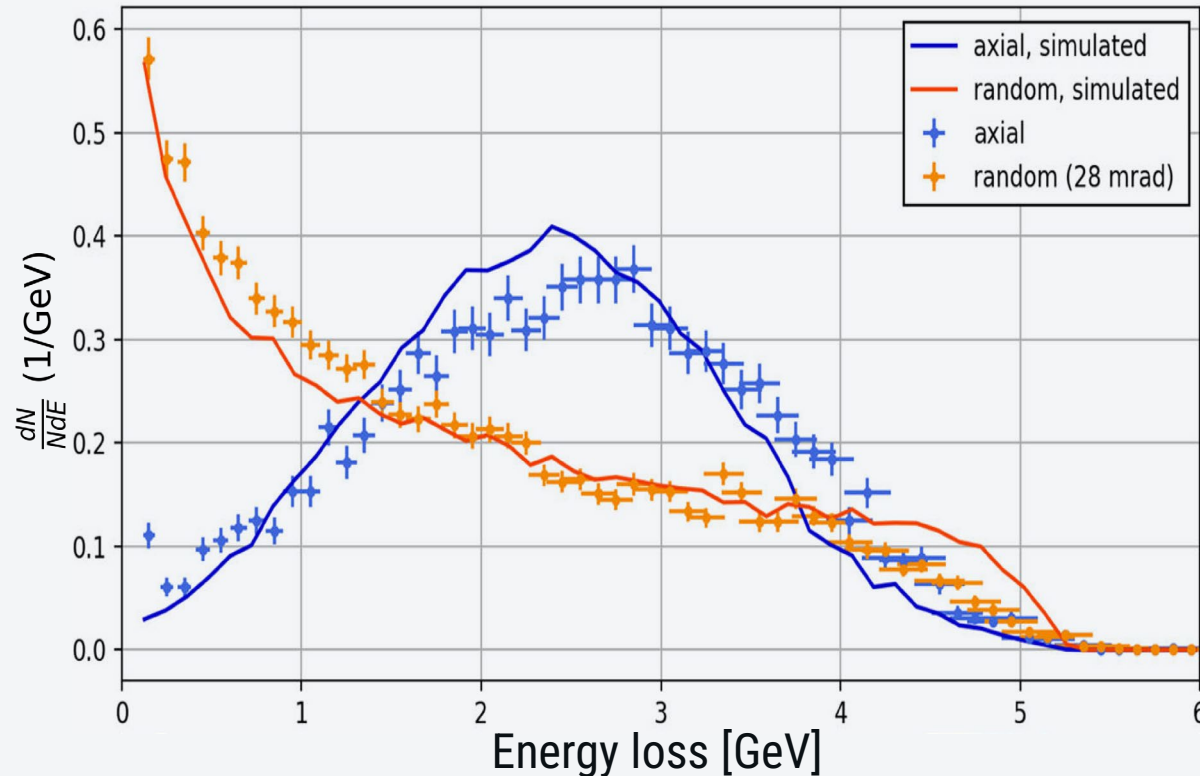
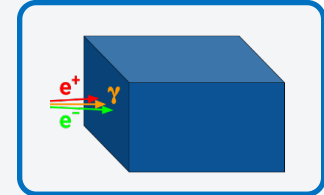


W of 2.25 mm (0.64 X0) aligned along $\langle 100 \rangle$ axis.

(research center manufactured crystal)

Radiated energy loss

Calorimeter Signal – Energy loss of
 W 2.25mm ($\sim 0.65X_0$) $\langle 001 \rangle$



Clear difference in energy loss distribution.
In axial orientation : **peaks above 2.5 GeV**,
In amorphous orientation it **vanishes** as typical for
Bremsstrahlung

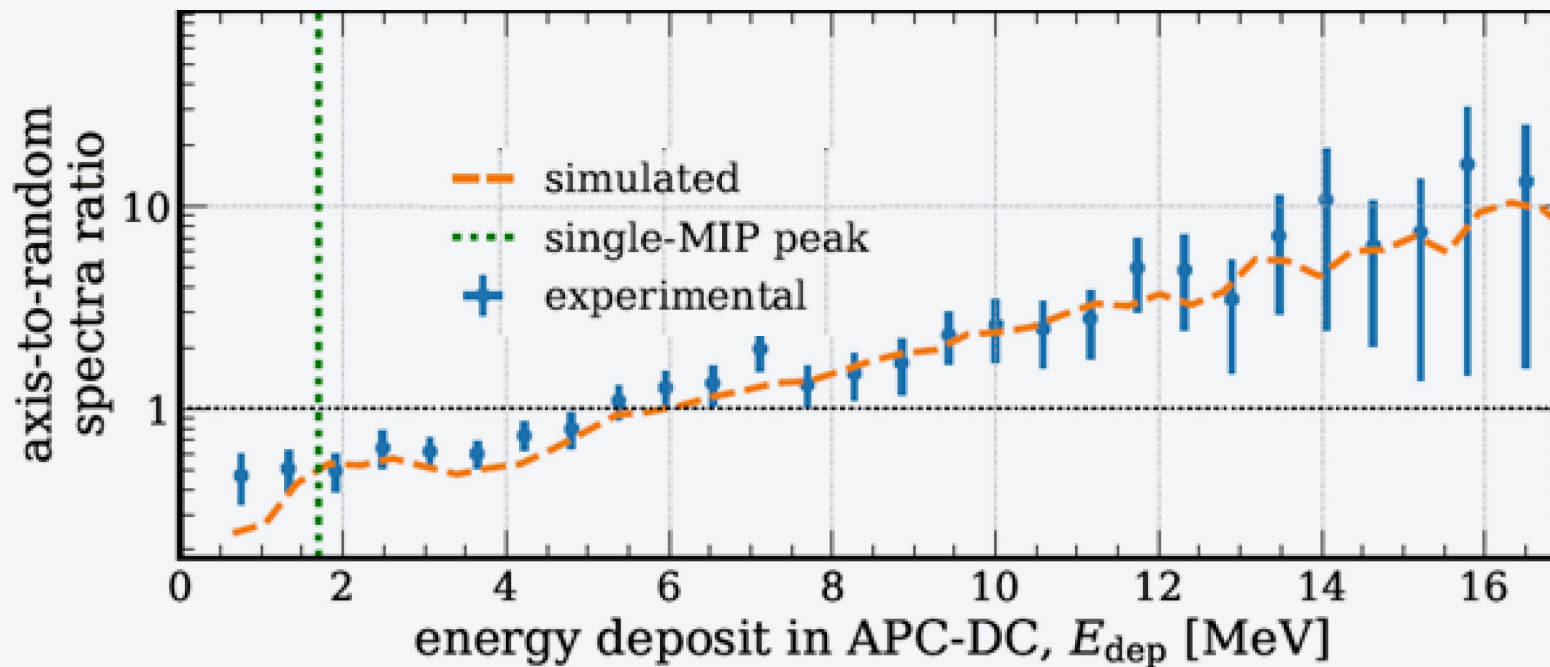
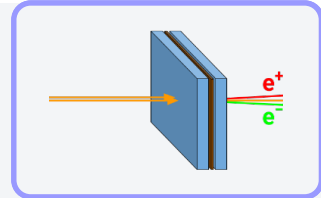
Bandiera et al. [4]

Active Photon Converter (APC)



DESY setup configuration

Active Photon Converter (Photon multiplicity counter)
axial to amorphous signal of W 2.25mm ($\sim 0.65X_0$) $\langle 001 \rangle$



Clear enhancement of photon production in axial orientation case

Bandiera et al. [4]

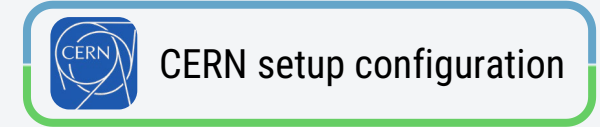
CERN PS

Electron beams at 6 GeV/c

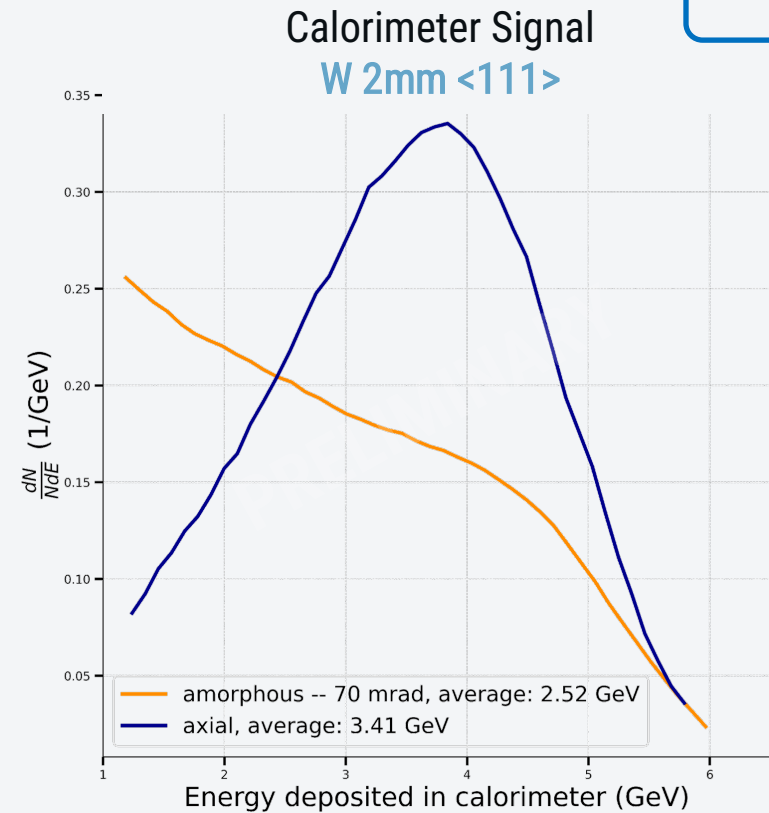
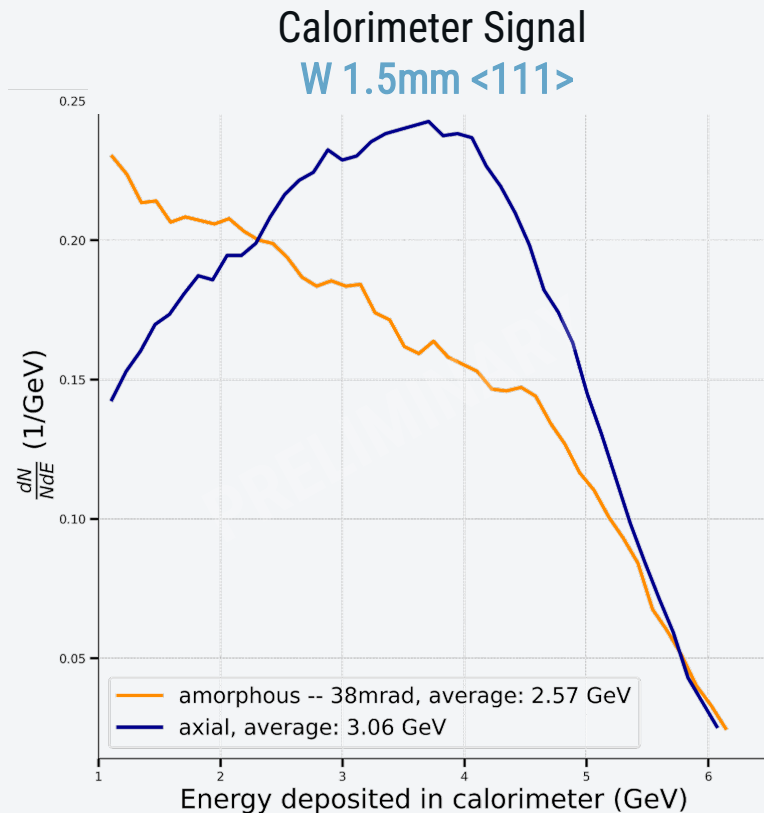
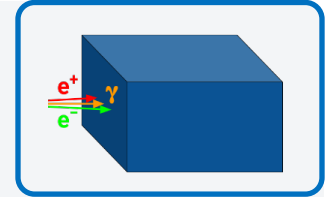


W of 1.5 - 2 mm (0.43 – 0.57 X_0) aligned along $\langle 111 \rangle$ axis. (industrial manufactured crystals)
 l_r of 1 - 2 mm (0.34 – 0.68 X_0) aligned along $\langle 110 \rangle$ axis. (industrial manufactured crystals)

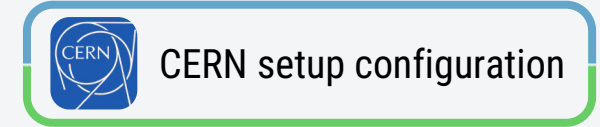
Radiated energy loss



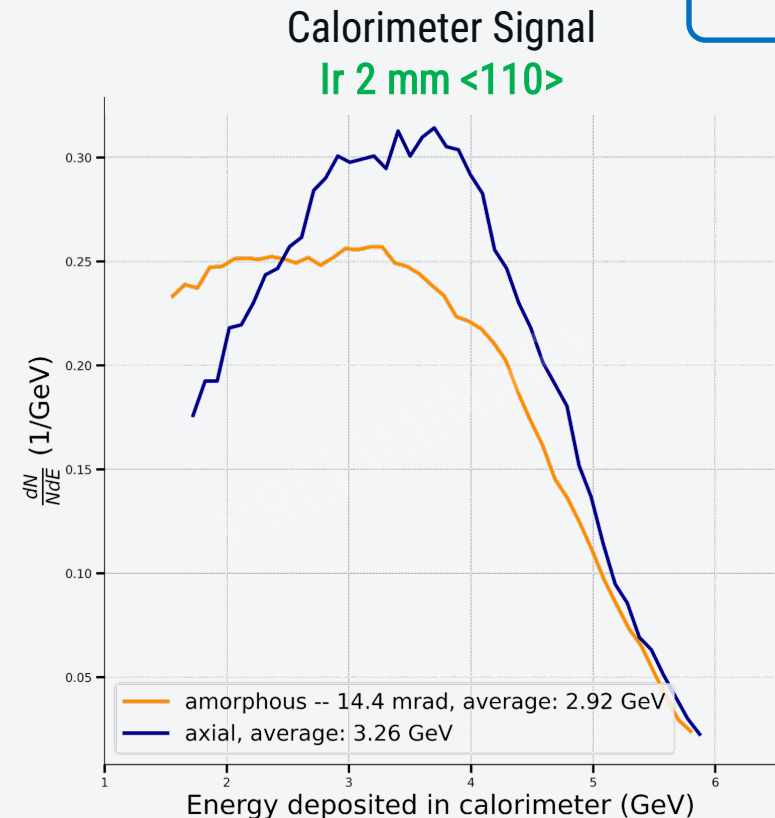
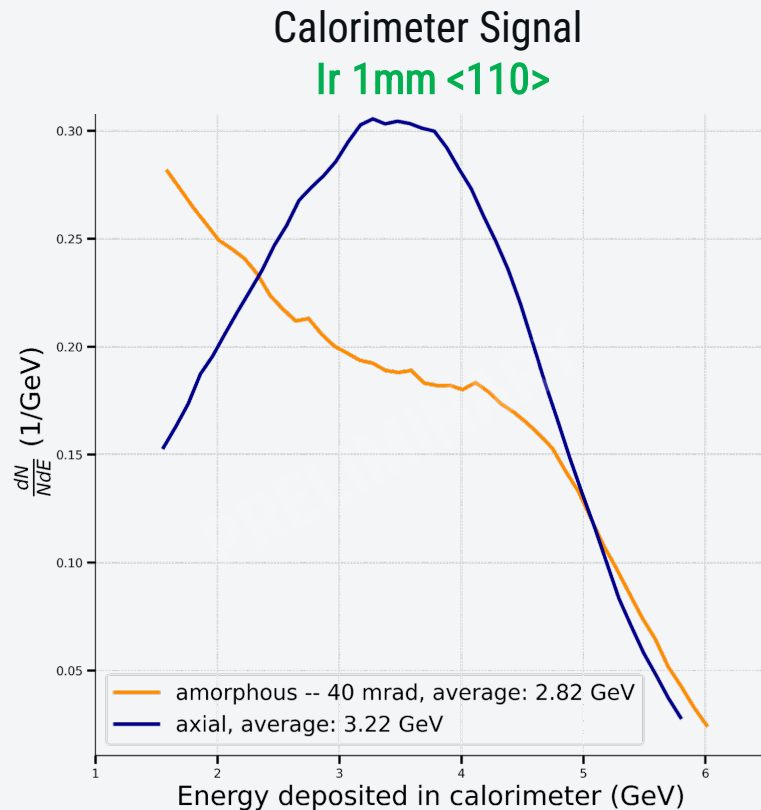
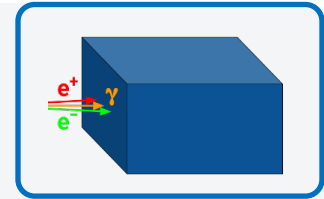
For both the **W** and **Ir** aligned along the **<111> axes** and the **<110> axes**, respectively, the radiative energy loss distribution **peaks above 3.5 GeV**, while for **amorphous orientation it vanishes** as typical for Bremsstrahlung



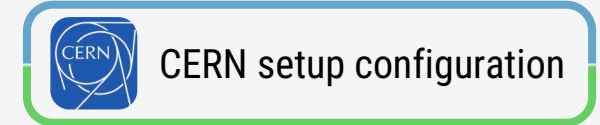
Radiated energy loss



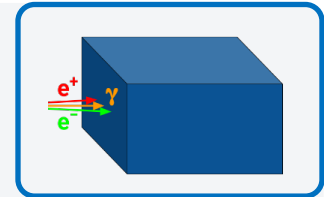
For both the **W** and **Ir** aligned along the **<111> axes** and the **<110> axes**, respectively, the radiative energy loss distribution **peaks above 3.5 GeV**, while for **amorphous orientation it vanishes** as typical for Bremsstrahlung



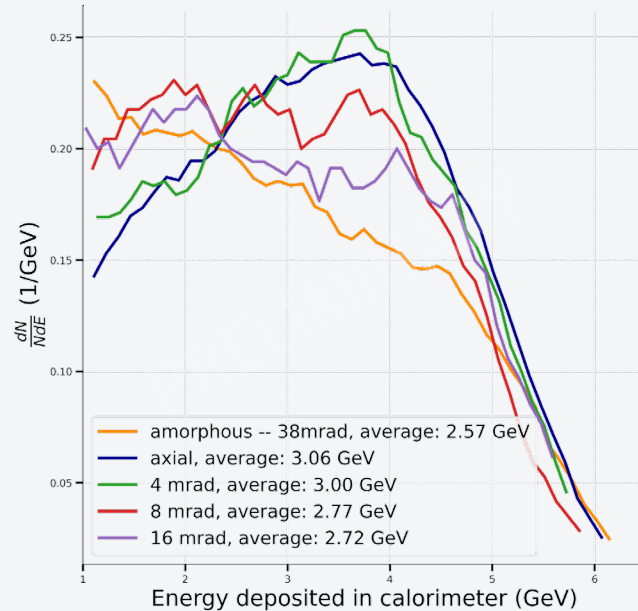
Radiated energy loss - Transition



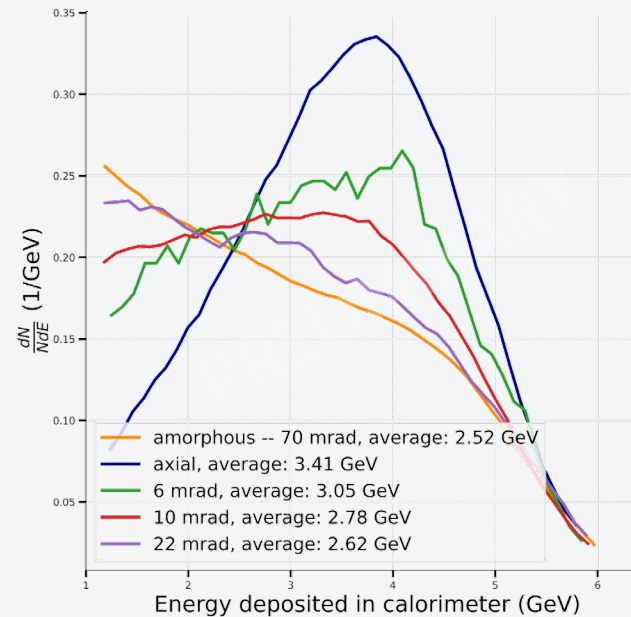
For both the **W** and **Ir** aligned along the **<111> axes** and the **<110> axes**, respectively, the radiative energy loss distribution peaks above 3.5 GeV, while for amorphous orientation it vanishes as typical for Bremsstrahlung



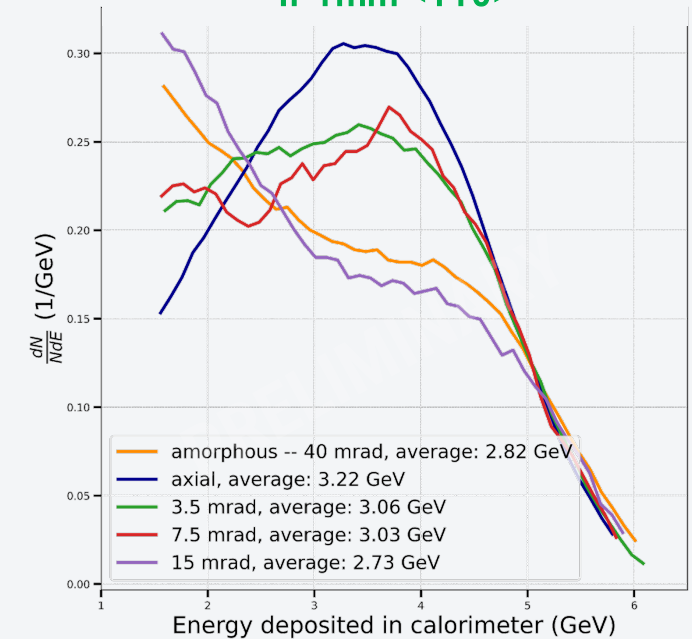
Calorimeter Signal
W 1.5mm <111>



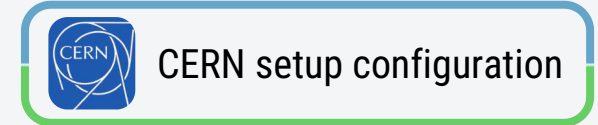
Calorimeter Signal
W 2mm <111>



Calorimeter Signal
Ir 1mm <110>

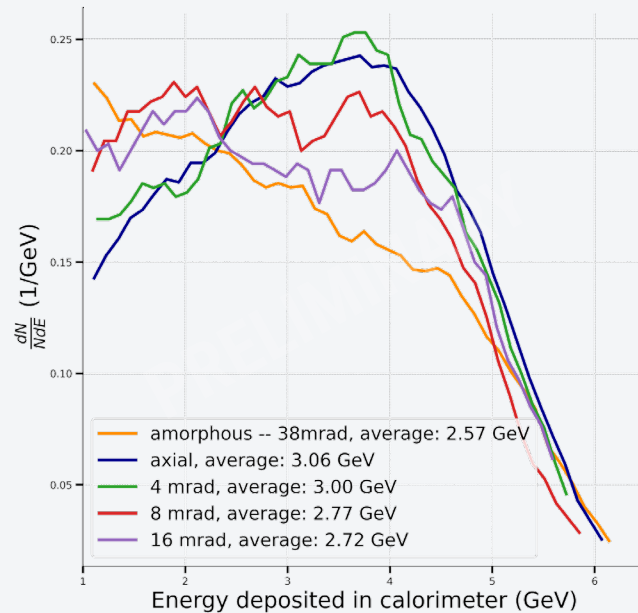


Radiated energy loss - Transition

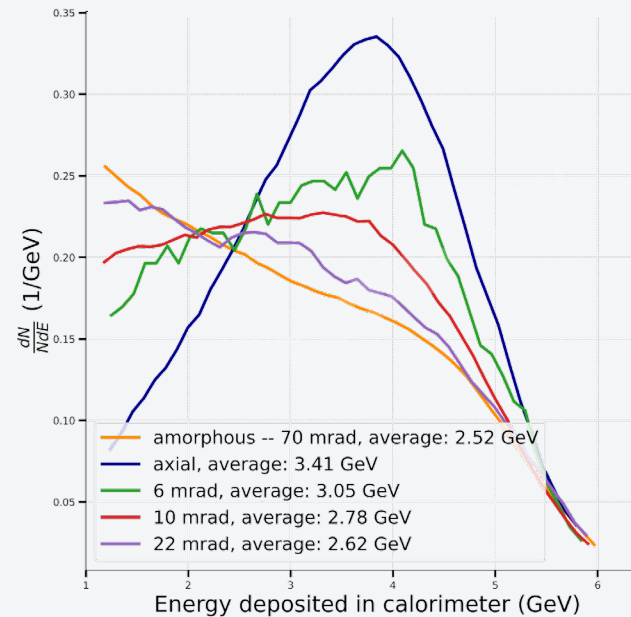


We observed continuous transition from amorphous to aligned mode with the axis, extending 15 mrad, *i.e.* much wider the critical angle (~ 0.6 mrad).

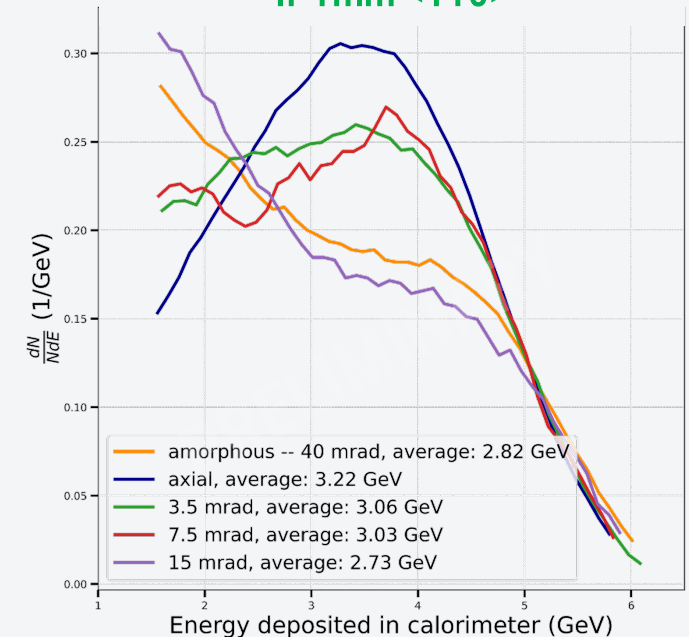
Calorimeter Signal
W 1.5mm <111>



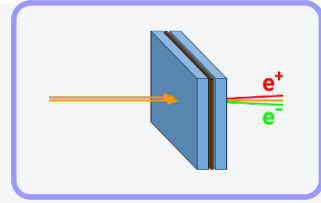
Calorimeter Signal
W 2mm <111>



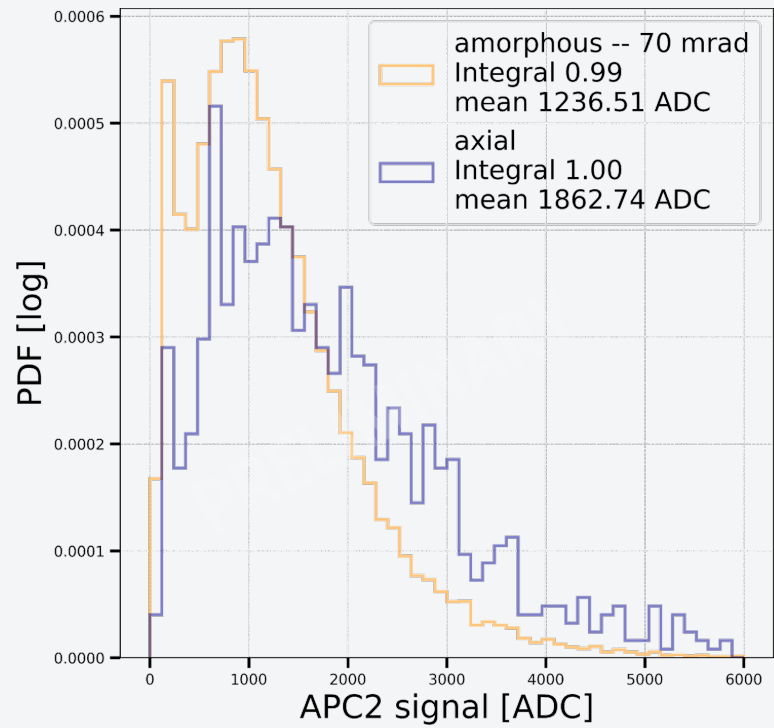
Calorimeter Signal
Ir 1mm <110>



Active Photon Converter (APC)



APC Signal
W 2 mm <111>

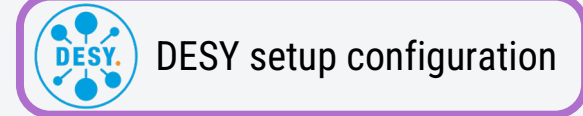


Clear enhancement of the energy deposited in the second scintillator, thus **more photon production** in axial orientation case

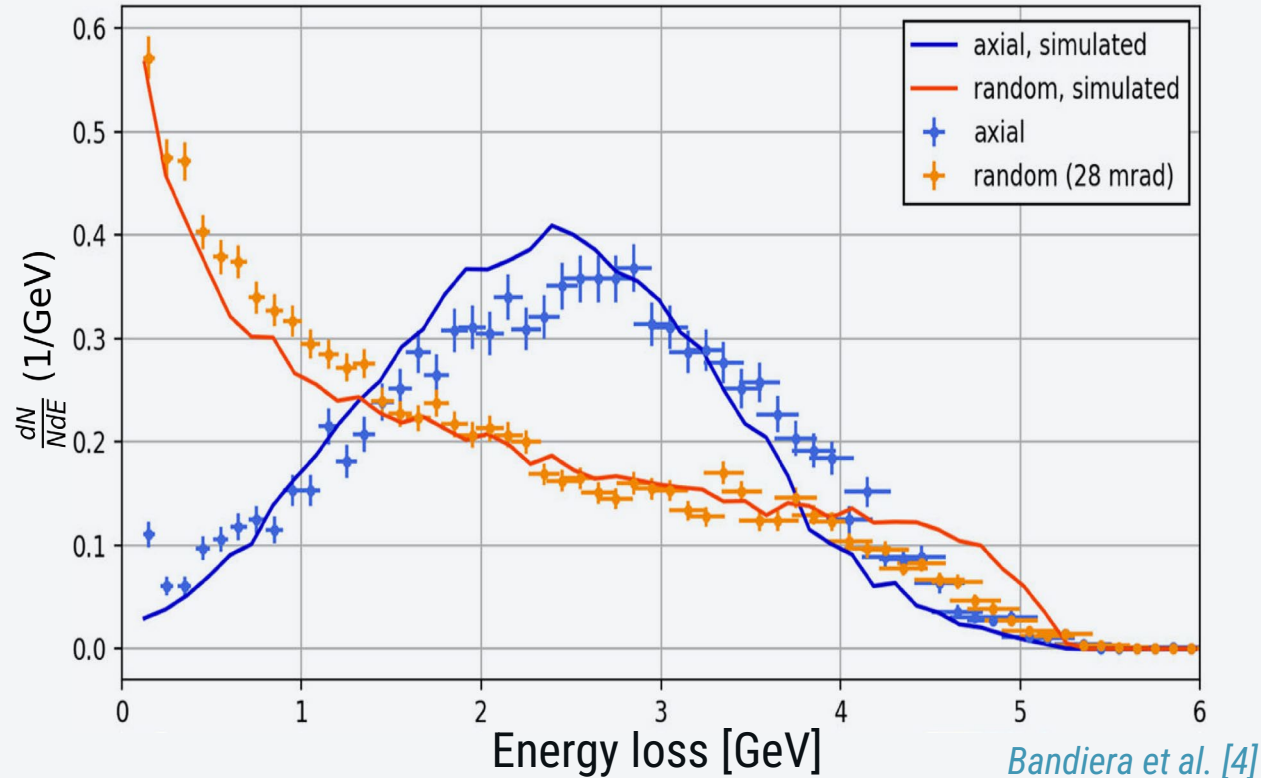
SIMULATION CODE VALIDATION



Our simulation code WORKS !



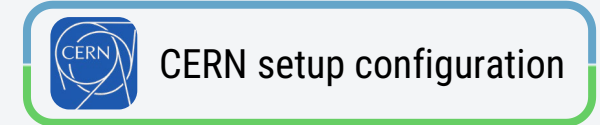
Calorimeter Signal – Energy loss of W 2.25mm ($\sim 0.65X_0$) $\langle 001 \rangle$



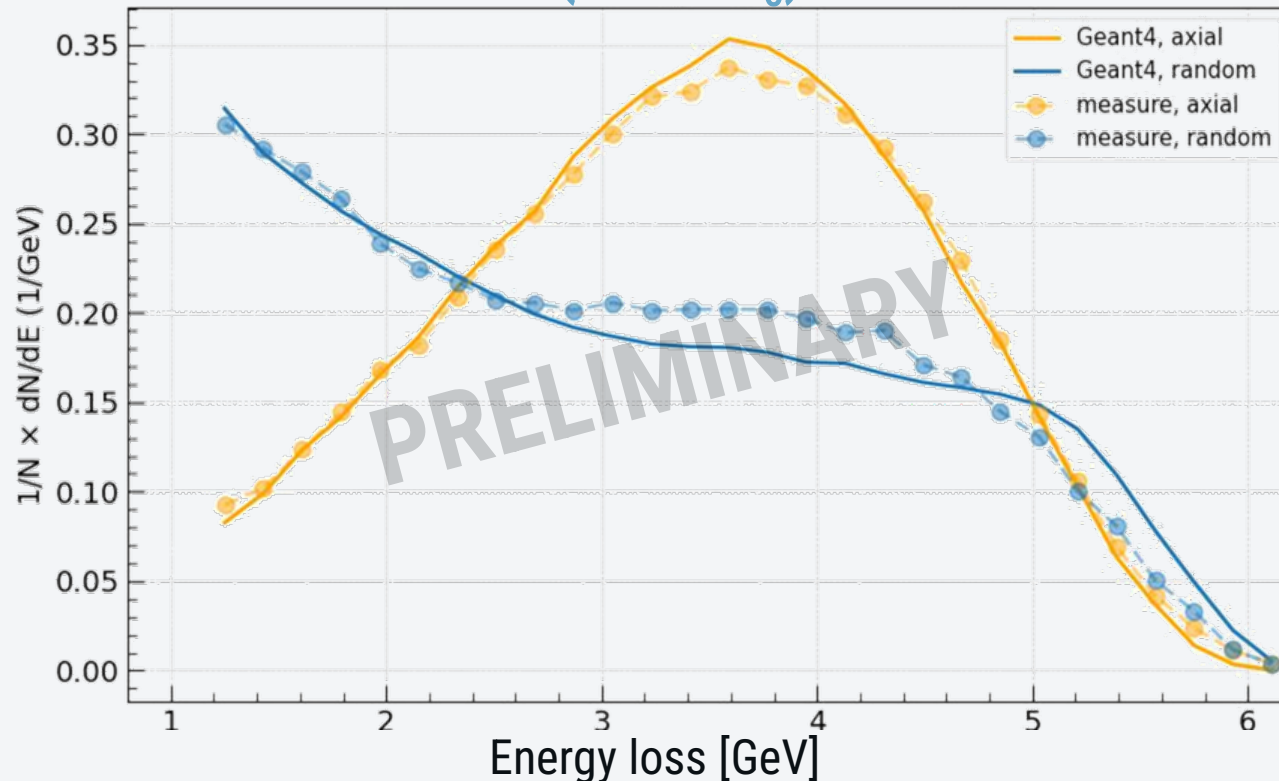
The results from beam tests conducted at DESY and CERN PS **agrees** with the Monte Carlo simulation:

- The whole setup was simulated using the Geant4 toolkit with the new *G4ChannelingFastSim* library
A. Sytov et al. [5 – 6]
- The output file encompassing all secondary γ and e^\pm particles considers the interactions within the entire experimental setup.
Bandiera et al. [4]

Our simulation code WORKS !



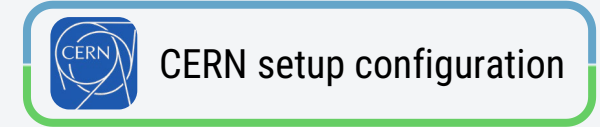
Calorimeter Signal – Energy loss of
 W 2mm ($\sim 0.57X_0$) $\langle 111 \rangle$



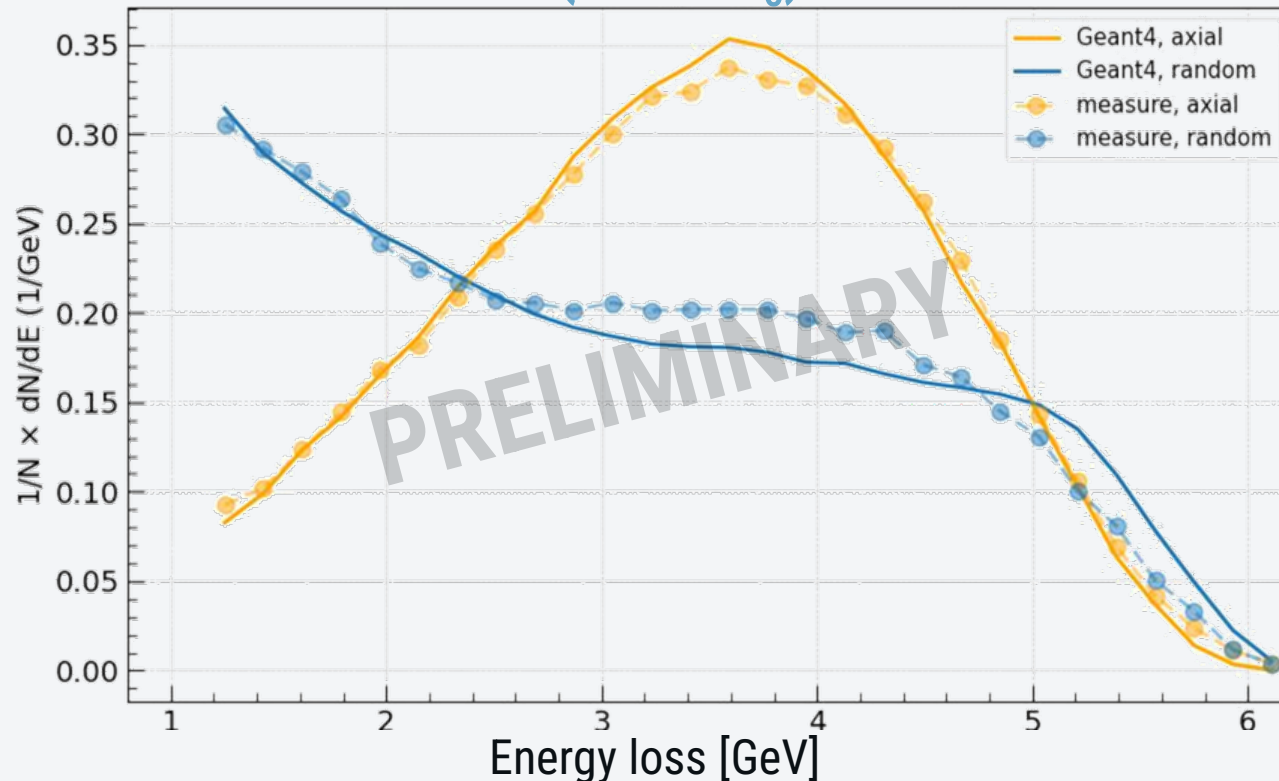
The results from beam tests conducted at DESY and CERN PS **agrees** with the Monte Carlo simulation:

- The whole setup was simulated using the Geant4 toolkit with the new *G4ChannelingFastSim* library
[A. Sytov et al. \[5 – 6\]](#)
- The output file encompassing all secondary γ and e^\pm particles considers the interactions within the entire experimental setup.
[Bandiera et al. \[4\]](#)

Our simulation code WORKS !



Calorimeter Signal – Energy loss of
 W 2mm ($\sim 0.57X_0$) $\langle 111 \rangle$



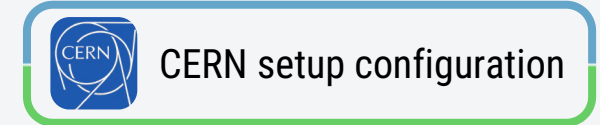
The results from beam tests conducted at DESY and CERN PS **agrees** with the Monte Carlo simulation:

- The whole setup was simulated using the Geant4 toolkit with the new *G4ChannelingFastSim* library
[A. Sytov et al. \[5 – 6\]](#)
- The output file encompassing all secondary γ and e^\pm particles considers the interactions within the entire experimental setup.
[Bandiera et al. \[4\]](#)

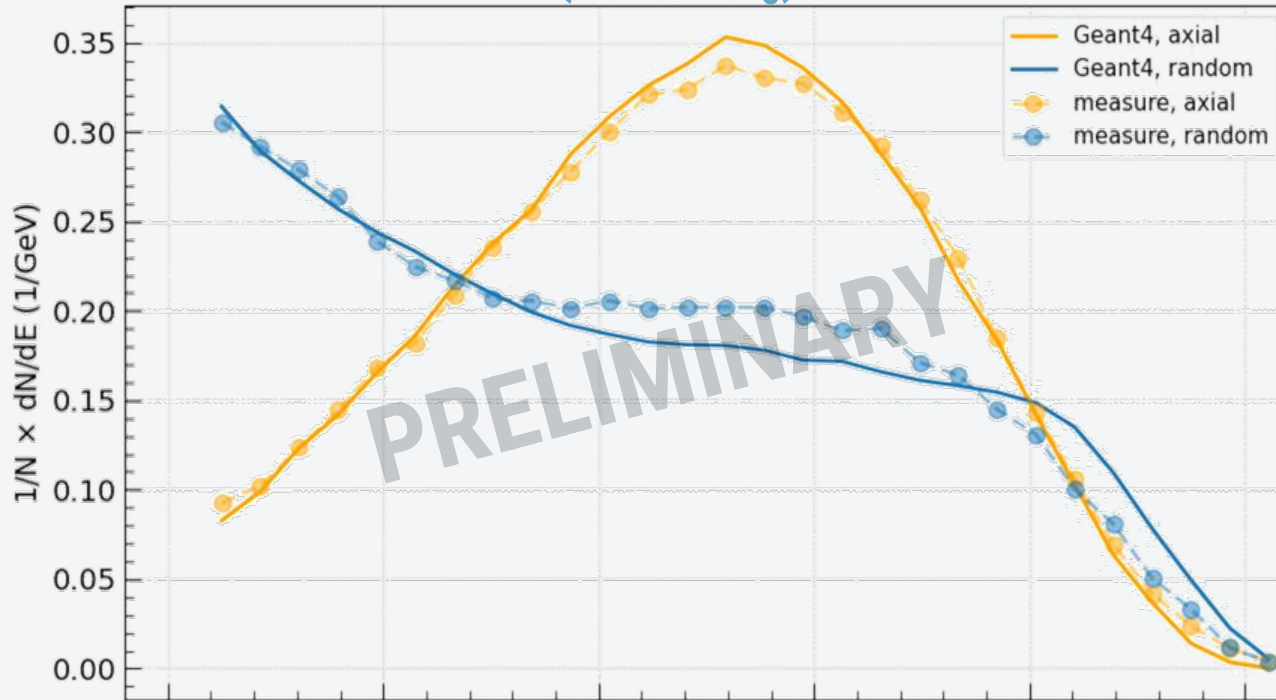
Once the **simulation environment was validated** against experimental findings, efforts were directed towards optimizing the FCC-ee positron source scheme.

Parameters chosen for the FCC-ee positron source optimization via Geant4

Our simulation code WORKS !



Calorimeter Signal – Energy loss of
 W 2mm ($\sim 0.57X_0$) $\langle 111 \rangle$



As seen in A. Sytov and G.Paternò
talks of 05/11/2024

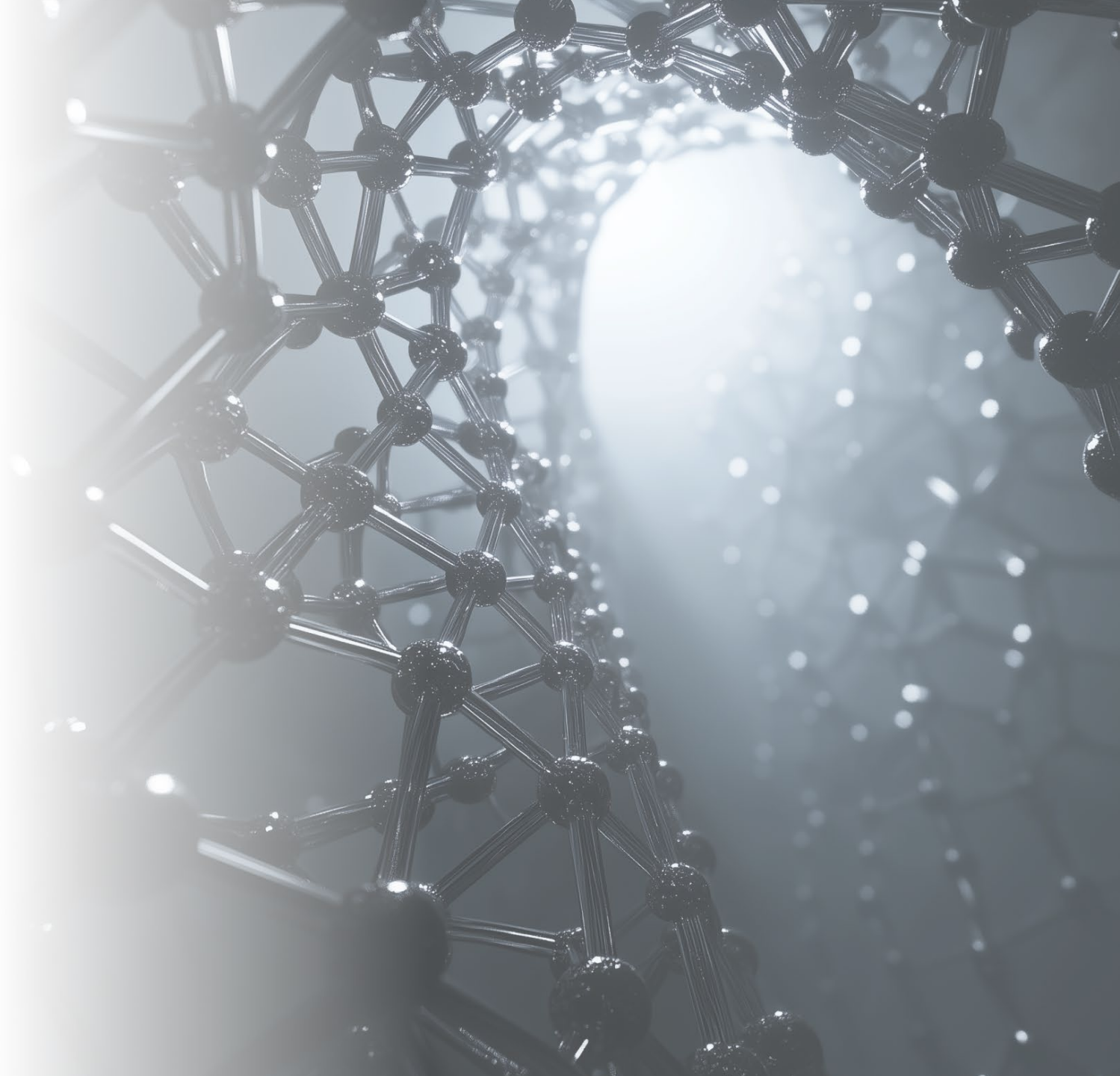
The results from beam tests conducted at DESY and CERN PS **agrees** with the Monte Carlo simulation:

- The whole setup was simulated using the Geant4 toolkit with the new *G4ChannelingFastSim* library
[A. Sytov et al. \[5 – 6\]](#)
- The output file encompassing all secondary γ and e^\pm particles considers the interactions within the entire experimental setup.
[Bandiera et al. \[4\]](#)

Once the **simulation environment was validated** against experimental findings, efforts were directed towards optimizing the FCC-ee positron source scheme.

Parameters chosen for the FCC-ee positron source optimization via Geant4

FUTURE PERSPECTIVE



Future Perspective

- Comparison with simulations:
 - W 1.5 mm
 - Ir
- Optimization of the hybrid source for 2.86 GeV/c

- Future test at CERN PS
 - New energy baseline (e^- 2.86 GeV/c)
 - Single crystal

Future Perspective

- Comparison with simulations:
 - W 1.5 mm
 - Ir
- Optimization of the hybrid source for 2.86 GeV/c

- Future test at CERN PS
 - New energy baseline (e^- 2.86 GeV/c)
 - Single crystal

Optimization of hybrid and single crystal including test of radiator converter for CHART P3 project





Further contact:

Laura Bandiera (INFN-Ferrara)
bandiera@fe.infn.it



ncanale@fe.infn.it

Iryna Chaikovska (IJCLab)
iryna.chaikovska@ijclab.in2p3.fr

References and Acknowledgment

References:

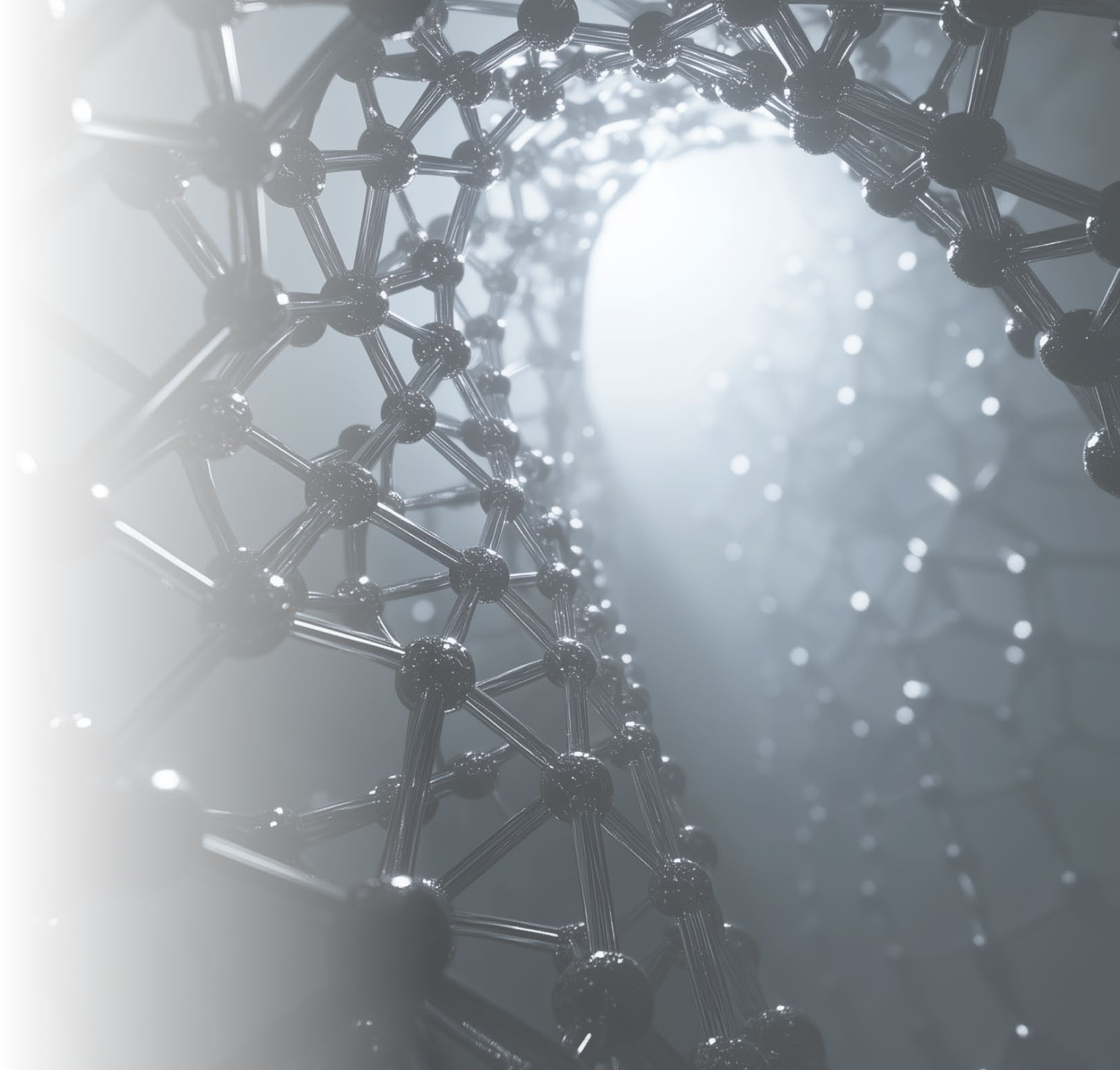
- [1] Frank Zimmermann, FCC Week 2024 10-14 June
- [2] R. Chehab et al., NIM B 266 (2008)
- [3] X. Artru, I. Chaikovska, R. Chehab et al. NIM B 355 (2015)
- [4] L. Bandiera et al., Eur. Phys. J. C 82 (2022)
- [5] A. Sytov et al. Phys. Rev. Accel. Beams 22 (2019)
- [6] A. Sytov et al. JKPS 83 (2023)

Acknowledgement:

We acknowledge financial support under the National Recovery and Resilience Plan (NRRP), Call for tender No. 104 published on 02.02.2022 by the Italian Ministry of University and Research (MUR), funded by the European Union – NextGenerationEU – Project Title : "*Intense positron source Based On Oriented crySTals - e+BOOST*" 2022Y87K7X – CUP I53D23001510006



BACKUP



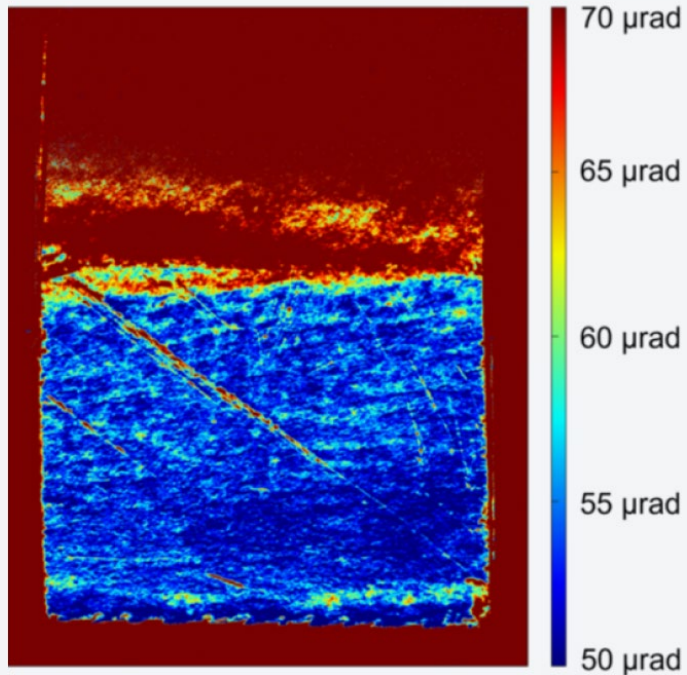


CRYSTAL CHARACTERIZATION

Research center crystals quality check



W 2.25mm
($\sim 0.65X_0$)
<001>



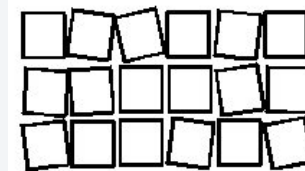
Imaging of the sample mosaicity measured at BM05 beamline of ESRF.

Color indicates the mosaicity of the sample

Characterization of mosaicity of the lattice performed at ESR Synchrotron (Grenoble, France)
(20 keV X rays)

Mosaicity $\leq 60 \mu\text{rad}$.

largest mosaicity are still below 150 μrad near the scratches

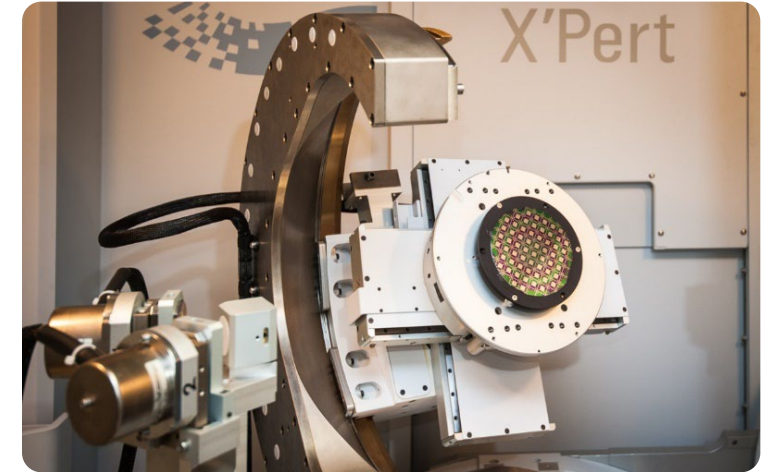


In crystallography, the *mosaicity* is a measure of the spread of crystal plane orientations

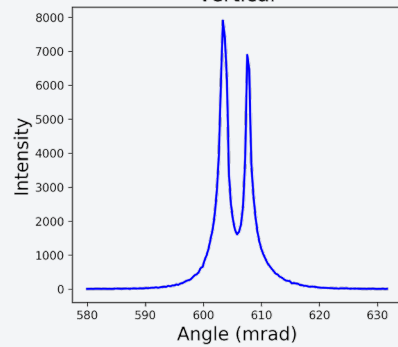
Industrial crystals quality check



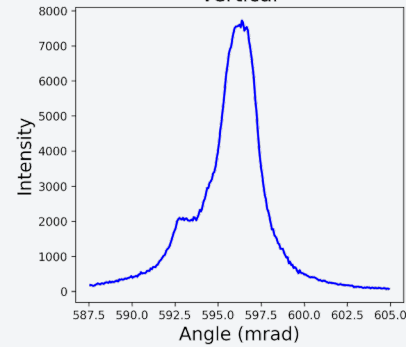
Characterization of superficial mosaicity of the lattice performed with High Resolution XRD at laboratories of Ferrara (@ 8.04 keV)



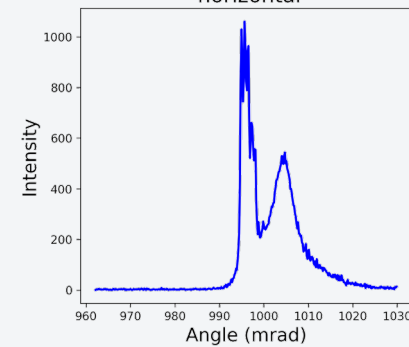
Ir <110> 1 mm
vertical



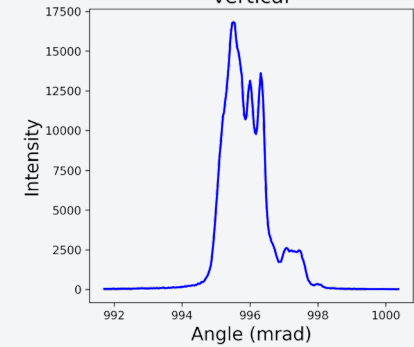
Ir <110> 2 mm
vertical



W <111> 1.5 mm (1)
horizontal



W <111> 2 mm
vertical

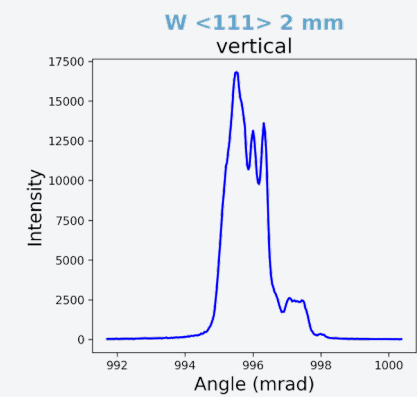
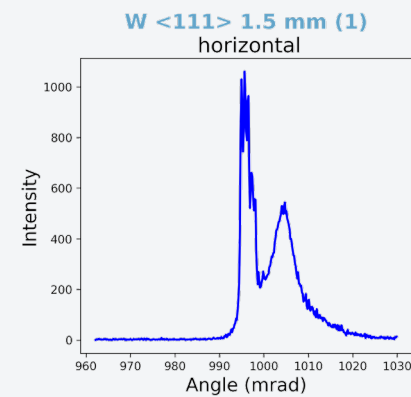
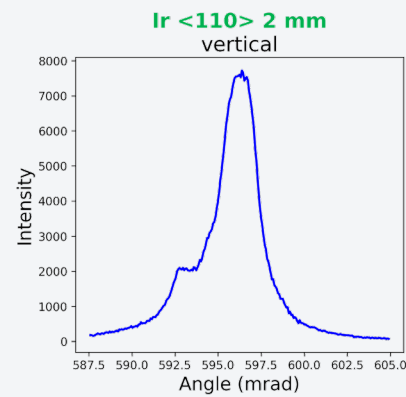
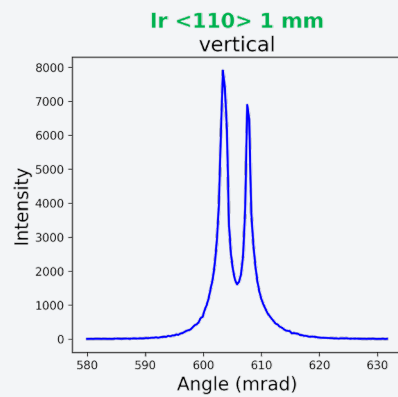
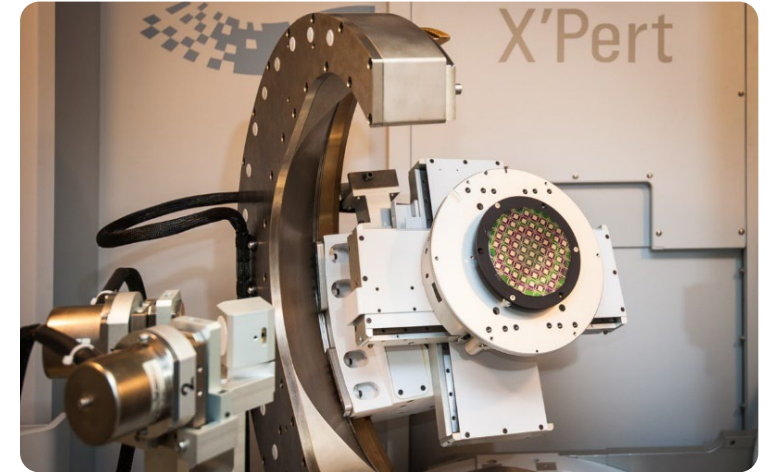


Industrial crystals quality check

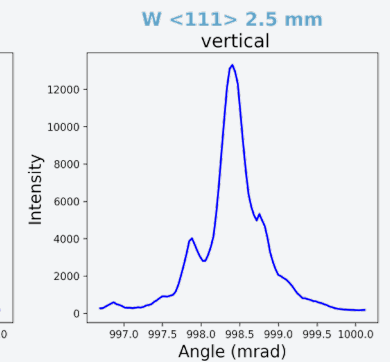
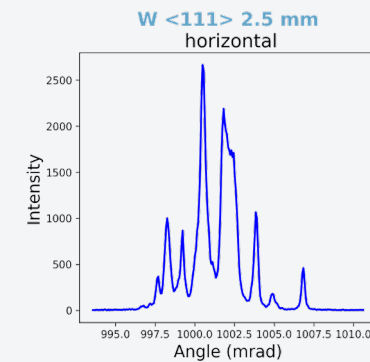
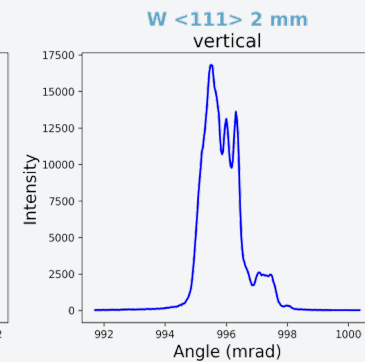
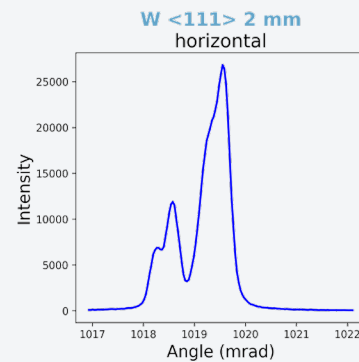
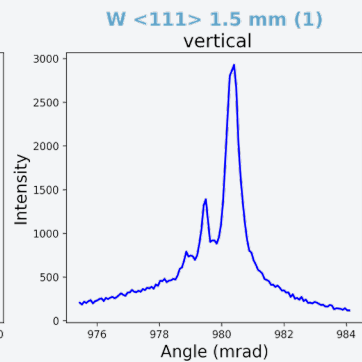
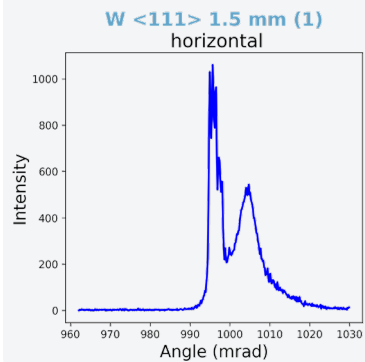
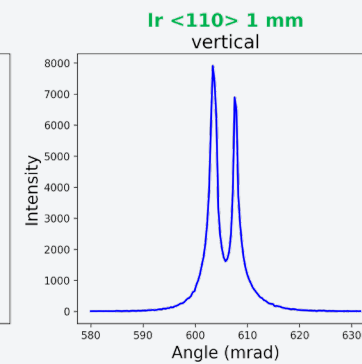
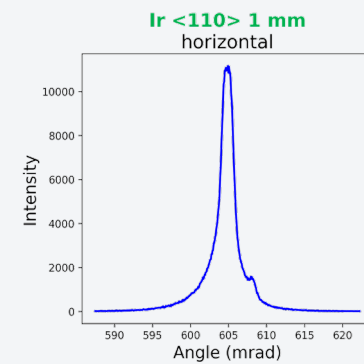
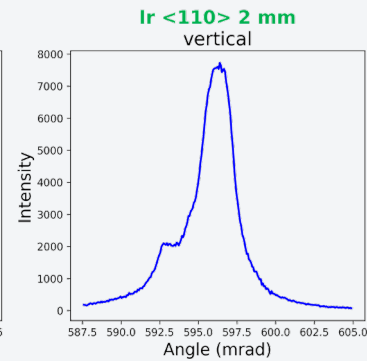
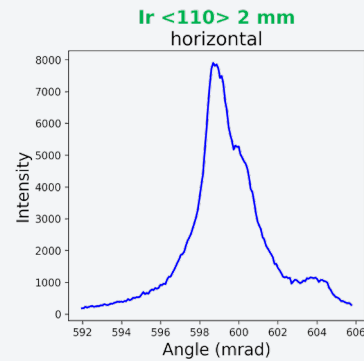


Characterization of superficial mosaicity of the lattice performed with High Resolution XRD at laboratories of Ferrara (@ 8.04 keV)

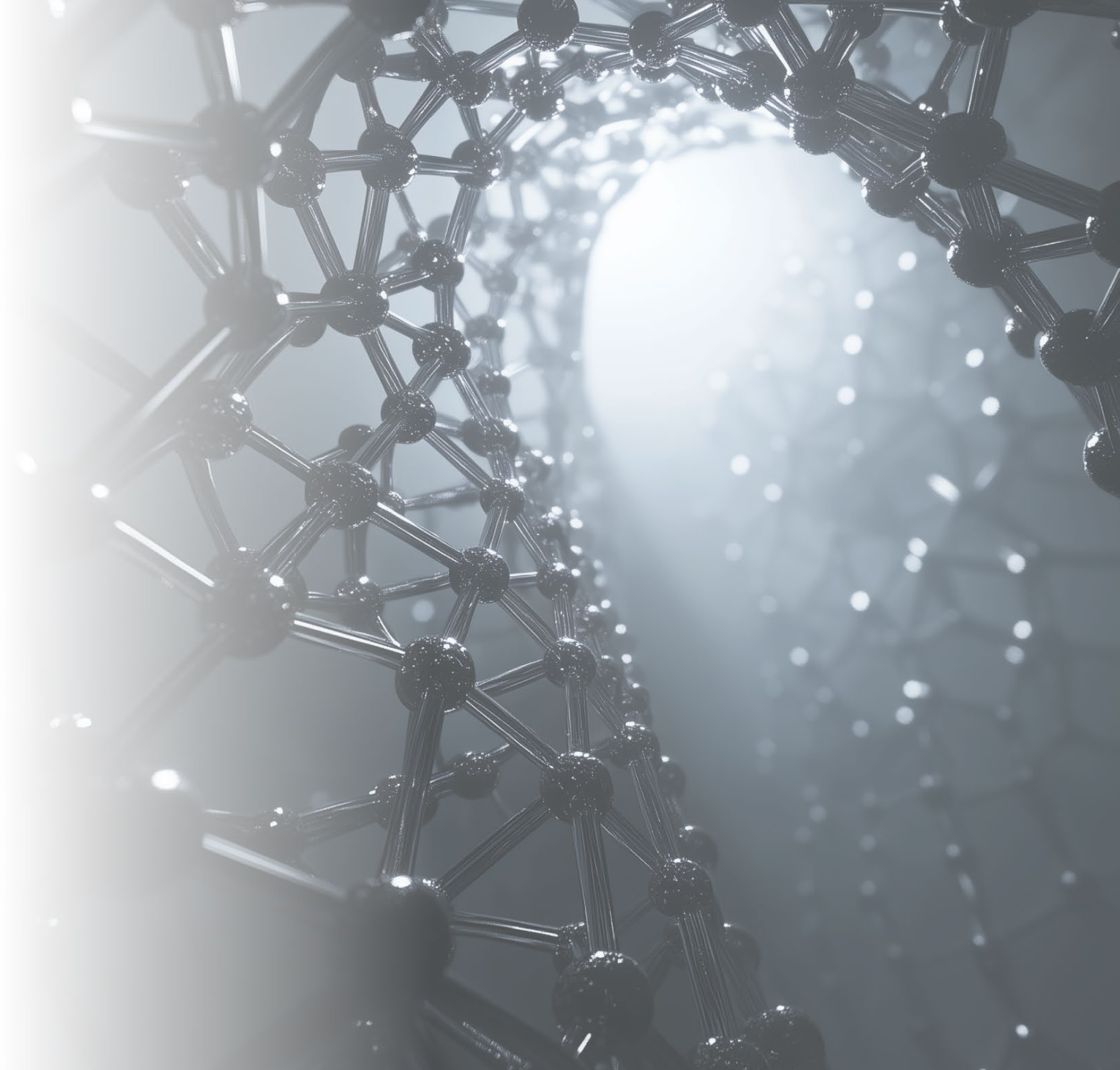
FWHM of industrial crystal is wider than the critical angle, the coherent effects are still available?



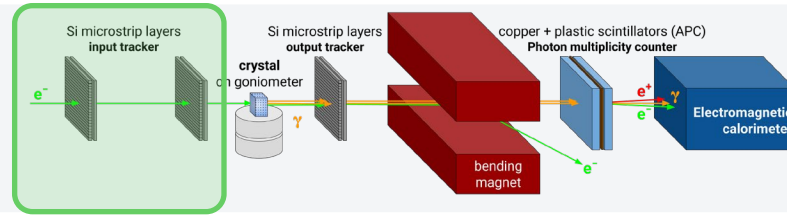
Summary of HRXRD test for CERN samples



INPUT TRACKERS

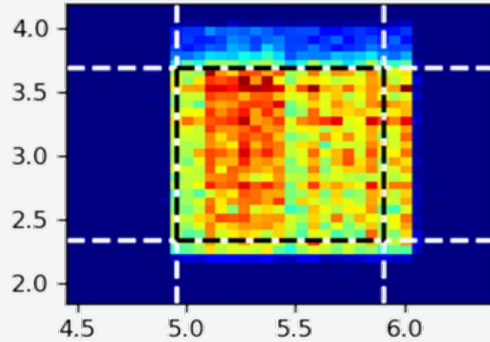


The setup

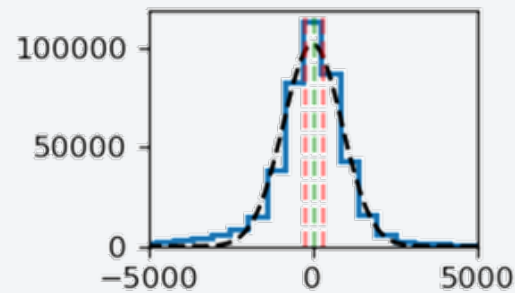


Input stage
Reconstruct track and
impinging angle on the crystal

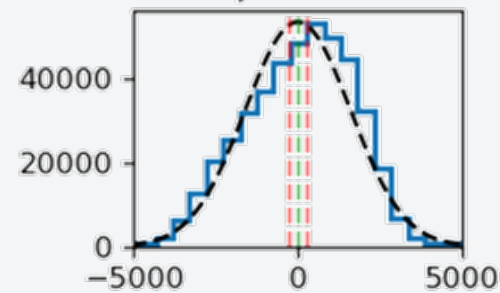
Chamber 2 position map



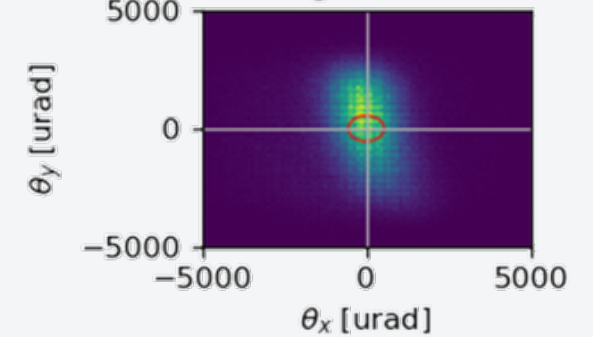
$\theta_{x,in}$ axial



$\theta_{y,in}$ axial



divergence axial

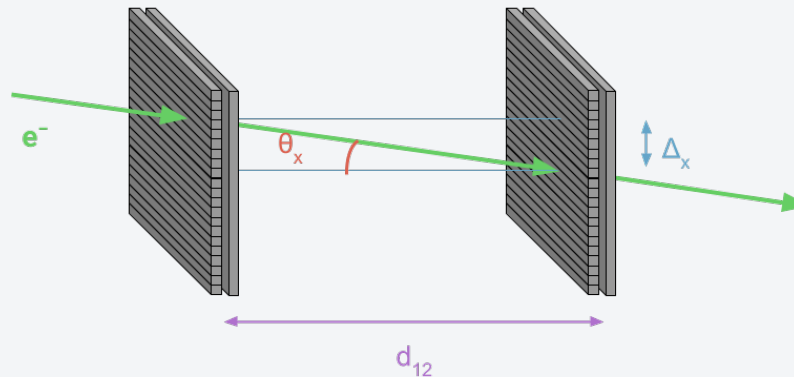


Hit position on Chamber weighted by Calo signal

input tracker

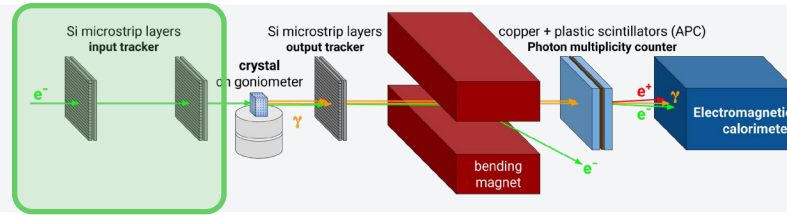
$\sim 2 \times 2$ or 9.5×9.5 cm² xy double-sided Si microstrip sensors, with an overall ~ 10 μm single-hit resolution self-triggering on strip to select the proper area

ϑ_{IN} reconstructed at crystal entrance



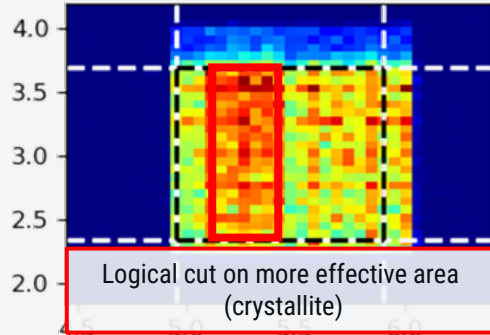
$$\vartheta_x = \arctan(\Delta_x / d_{12})$$

The setup

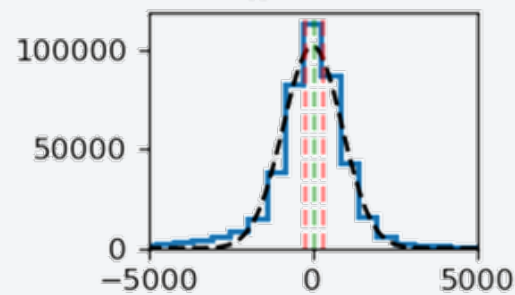


Input stage
Reconstruct track and
impinging angle on the crystal

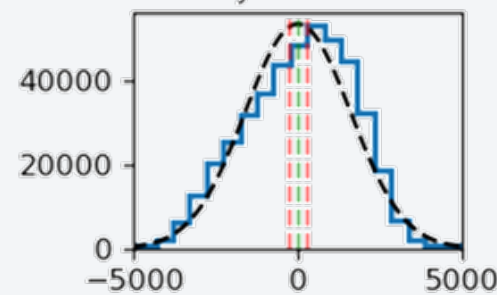
Chamber 2 position map



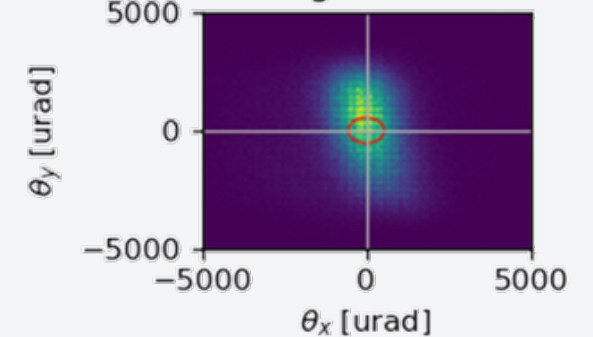
$\theta_{x \text{ in axial}}$



$\theta_{y \text{ in axial}}$



divergence axial

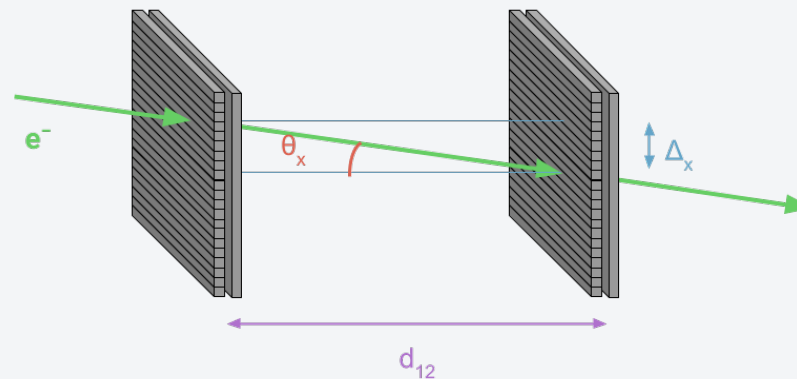


Hit position on Chamber weighted by Calo signal

input tracker

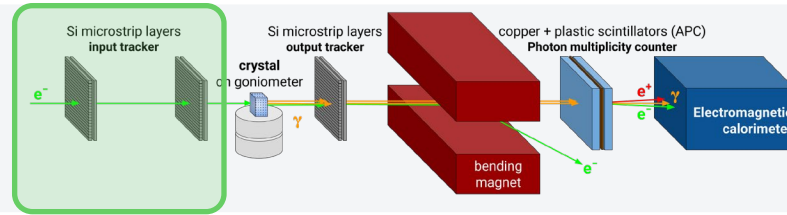
$\sim 2 \times 2$ or $9.5 \times 9.5 \text{ cm}^2$ xy double-sided Si microstrip sensors, with an overall $\sim 10 \mu\text{m}$ single-hit resolution self-triggering on strip to select the proper area

ϑ_{IN} reconstructed at crystal entrance



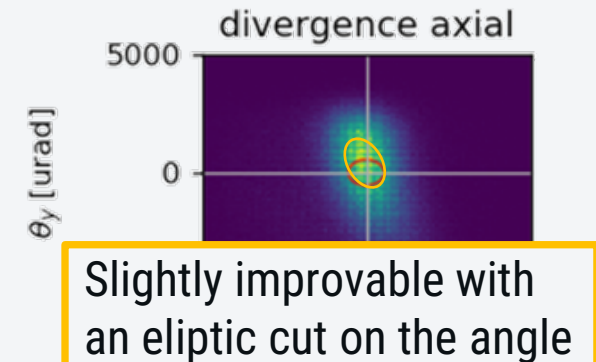
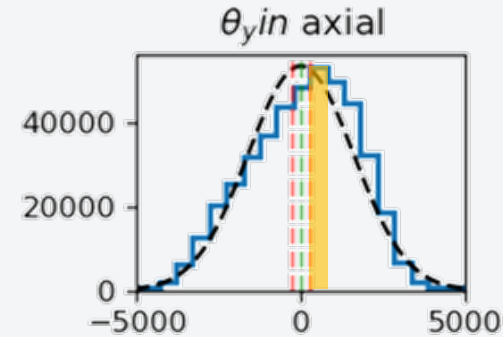
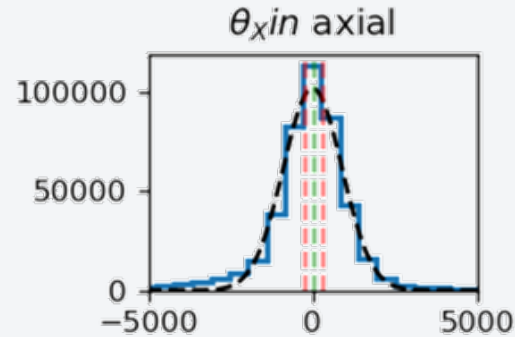
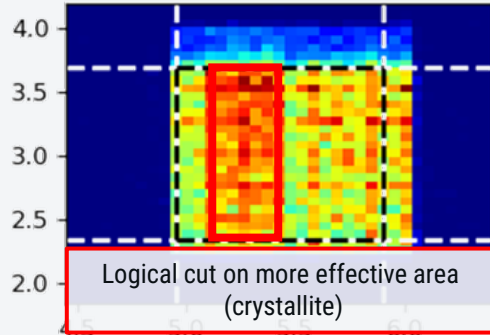
$$\vartheta_x = \arctan(\Delta_x / d_{12})$$

The setup



Input stage
Reconstruct track and
impinging angle on the crystal

Chamber 2 position map

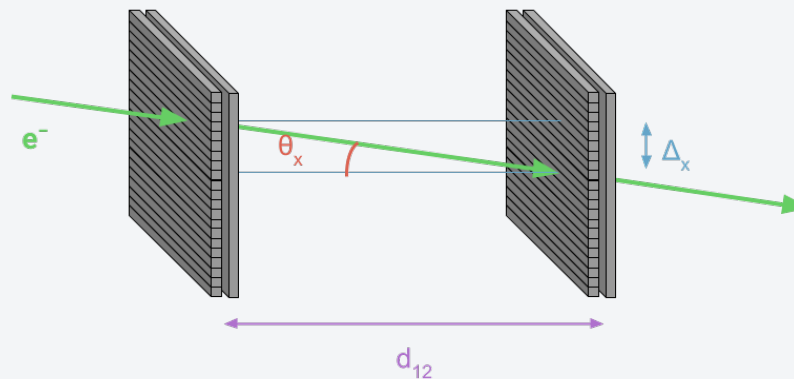


Hit position on Chamber weighted by Calo signal

input tracker

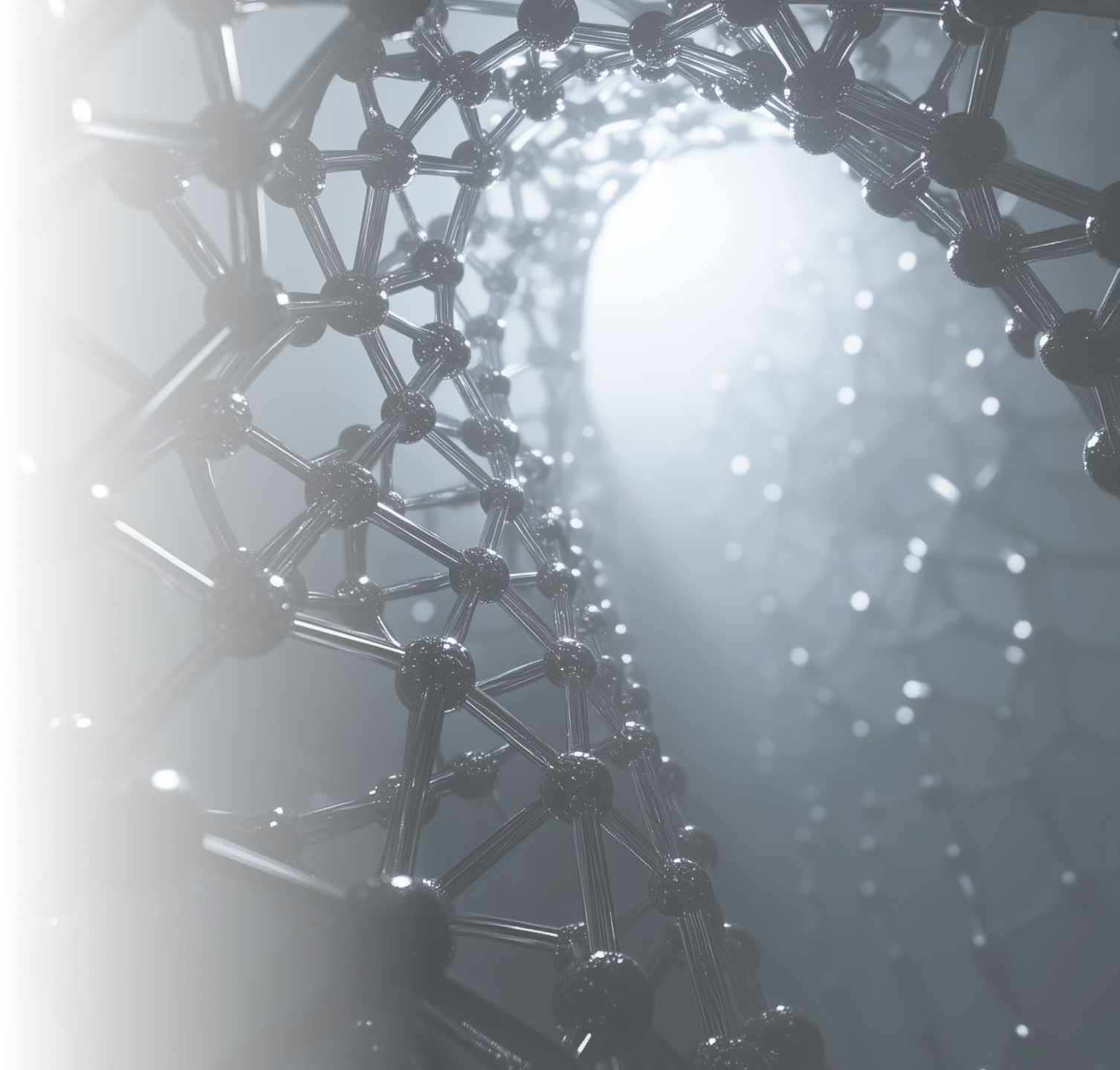
$\sim 2 \times 2$ or 9.5×9.5 cm² xy double-sided Si microstrip sensors, with an overall ~ 10 μ m single-hit resolution self-triggering on strip to select the proper area

ϑ_{IN} reconstructed at crystal entrance

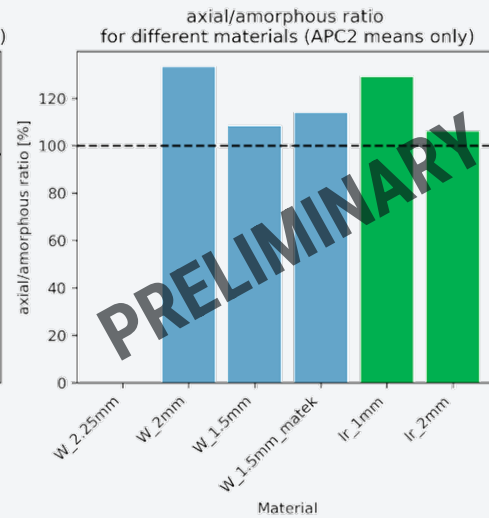
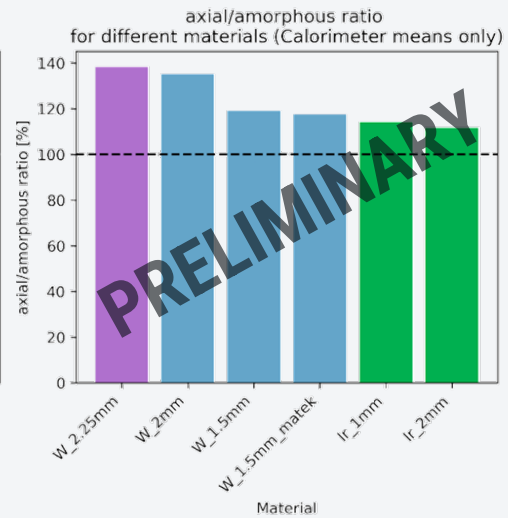
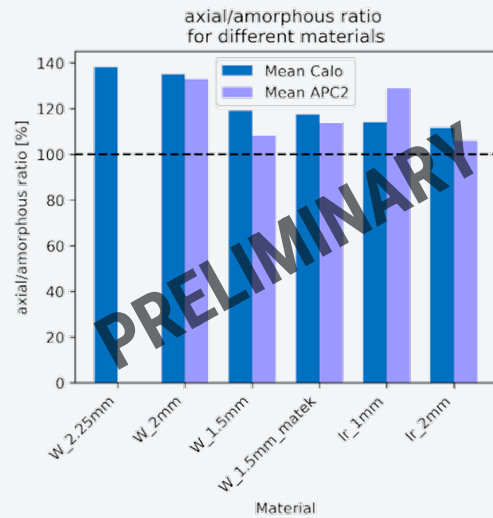


$$\vartheta_x = \arctan(\Delta_x / d_{12})$$

RESULTS SUMMARY



Summary



Material	Axial/amorph Calo	Axial/amorph APC2
Ir_1mm <110>	~114 %	~129 %
Ir_2mm <110>	~112 %	~106 %
W_1.5 mm <111>	~119 %	~108 %
W_2mm <111>	~135 %	~133 %
W_2.25 <100>	~138 %	Not calculated

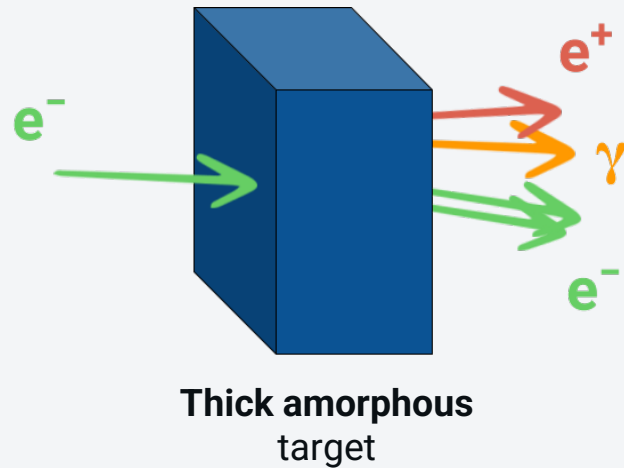


**CONVENTIONAL
 e^+ SOURCE PROBLEMS**

Conventional scheme limitations

As seen
in A.Sytov and
G.Paternò talks

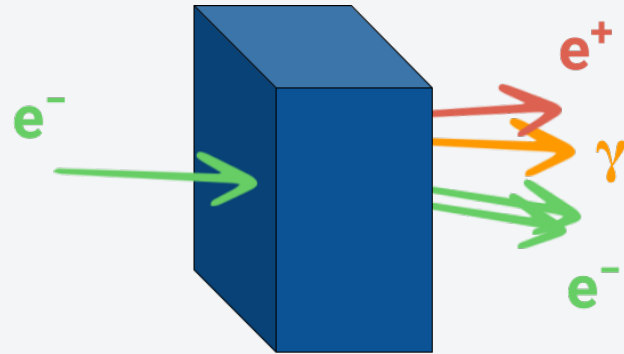
Conventional scheme



Conventional scheme limitations

As seen
in A.Sytov and
G.Paternò talks

Conventional scheme



Thick amorphous
target

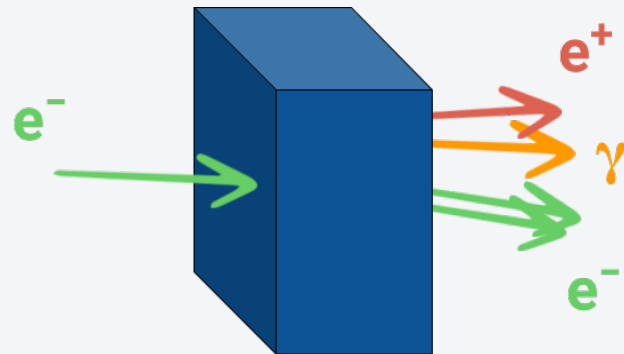
Current (Limited by the target)

- Average energy deposition
→ target heating/melting

Conventional scheme limitations

As seen
in A.Sytov and
G.Paternò talks

Conventional scheme



Thick amorphous
target

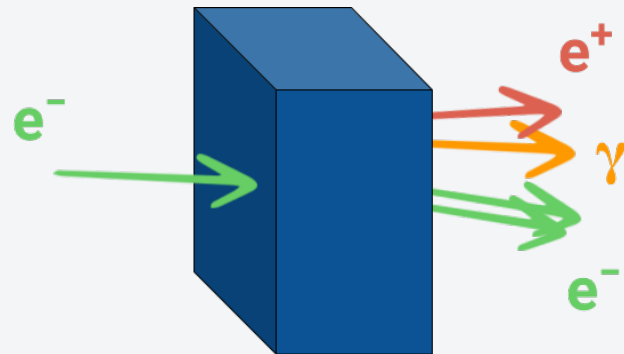
Current (Limited by the target)

- Average energy deposition
→ target heating/melting
- Peak Energy Deposition Density (PEDD)
→ Inhomogeneous and instantaneous energy deposition, that cause thermomechanical stresses due to temperature gradient

Conventional scheme limitations

As seen
in A.Sytov and
G.Paternò talks

Conventional scheme



Thick amorphous
target

Current (Limited by the target)

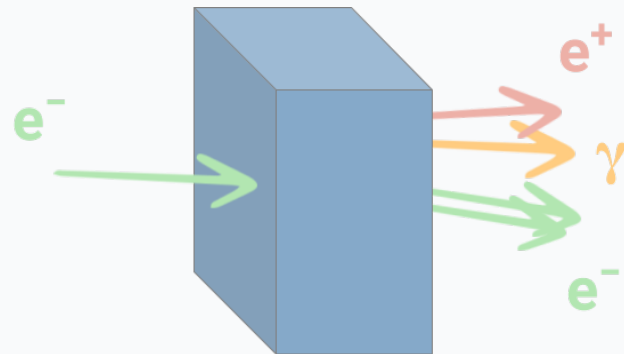
- Average energy deposition
→ target heating/melting
- Peak Energy Deposition Density (PEDD)
→ Inhomogeneous and instantaneous energy deposition, that cause thermomechanical stresses due to temperature gradient

**e^+ source set a critical constraint for the peak and average current → Luminosity Constraint!
Especially for future Linacs**

Hybrid crystal based positron source for e^-e^+ colliders

Idea of R. Chehab, A. Variola, V. Strakhovenko and X. Artru [3]

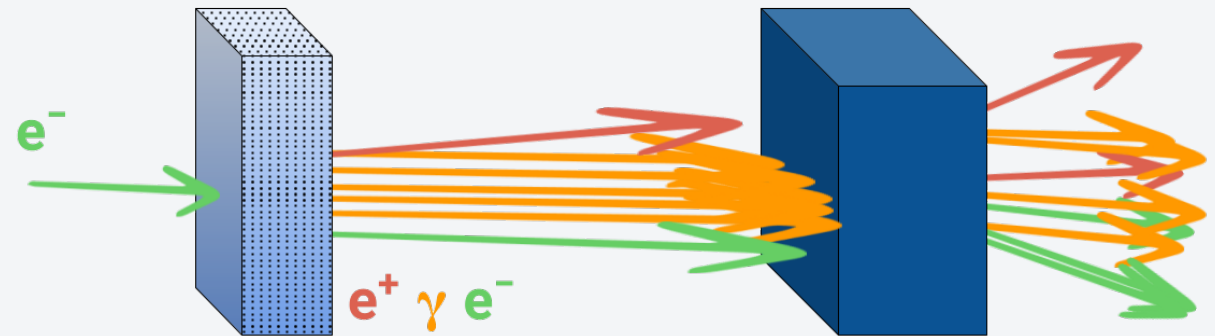
Conventional scheme



Thick amorphous target

Problem in future Linacs

Hybrid positron source



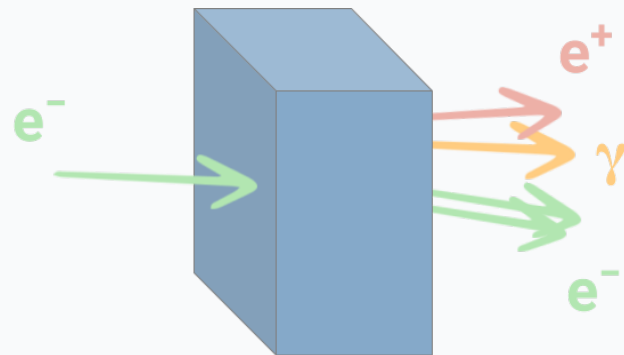
"Thin" oriented crystalline target ($< X_0$)
photon radiator

Amorphous target-converter

Hybrid crystal based positron source for e^-e^+ colliders

Idea of R. Chehab, A. Variola, V. Strakhovenko and X. Artru [3]

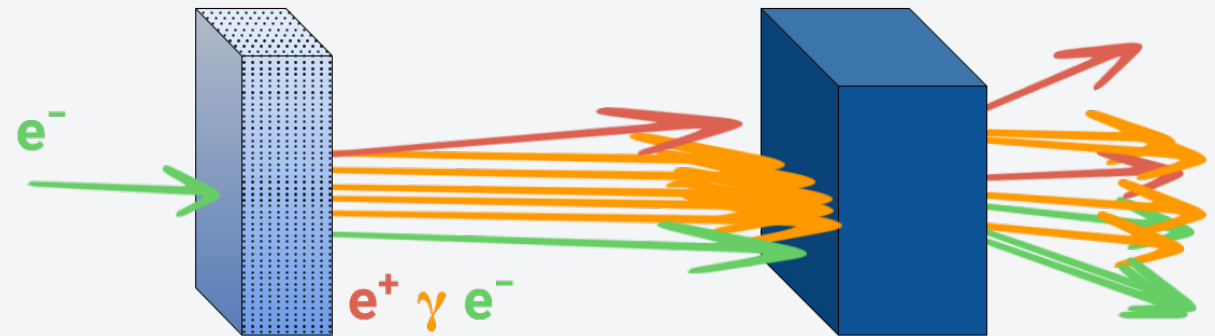
Conventional scheme



Thick amorphous target

Problem in future Linacs

Hybrid positron source



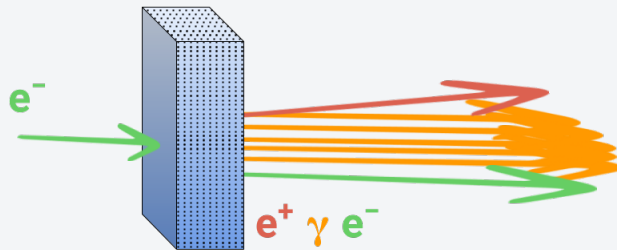
"Thin" oriented crystalline target ($< X_0$)
photon radiator

Amorphous target-converter

"Thin" crystal radiator, with thickness $< X_0$ will limit the heating, enhance the radiation and thus increase the target reliability

Coherent effects for crystal-based positron sources

Crystalline photon radiator



"Thin" oriented crystalline target ($< X_0$)
photon radiator

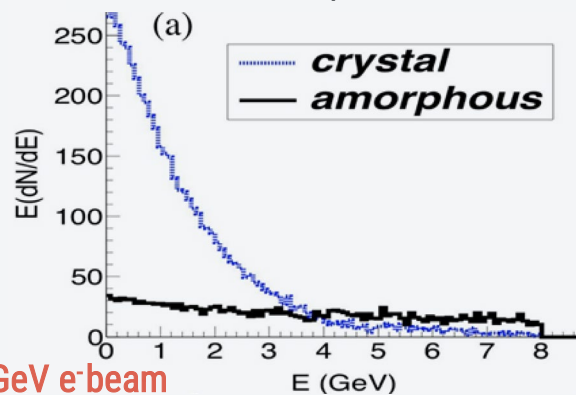
Hybrid positron source



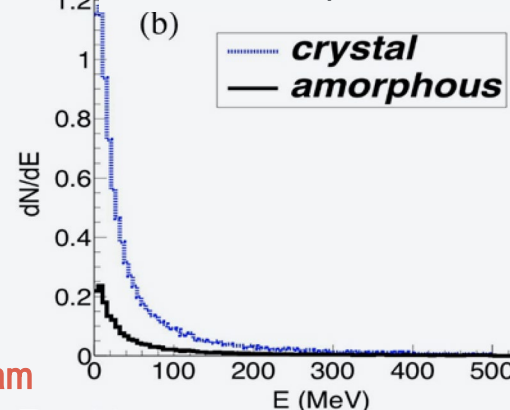
"Thin" crystal ($< X_0$)
photon radiator
Amorphous
target-converter

1. Enhancement of photon generation in crystals in coherent conditions \rightarrow enhancement of pair production in the converter target

Photon spectrum X. Artru et al. [3]

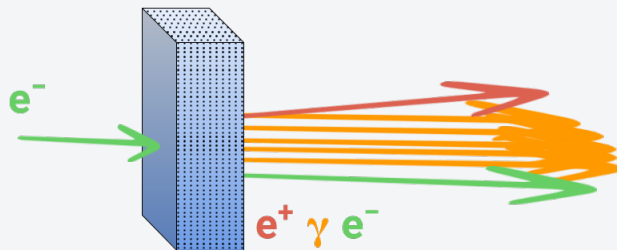


Positron spectrum X. Artru et al. [3]



Coherent effects for crystal-based positron sources

Crystalline photon radiator



"Thin" oriented crystalline target ($< X_0$)
photon radiator

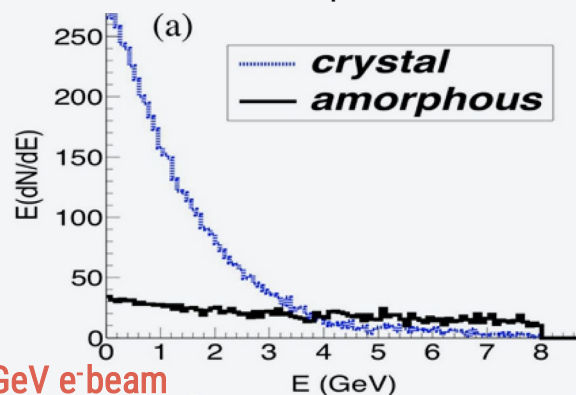
Hybrid positron source



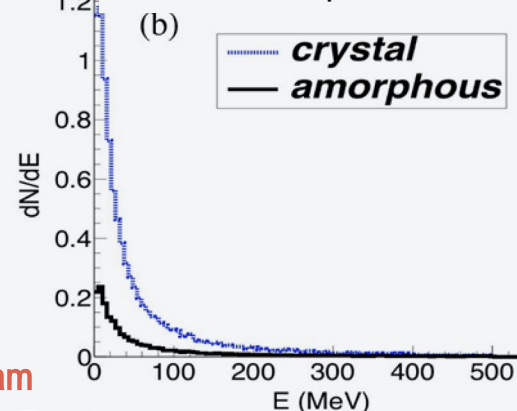
"Thin" crystal ($< X_0$)
photon radiator
Amorphous
target-converter

1. Enhancement of photon generation in crystals in coherent conditions \rightarrow enhancement of pair production in the converter target
2. High rate of soft photons \rightarrow creation of soft e^+ easily captured in matching systems

Photon spectrum X. Artru et al. [3]

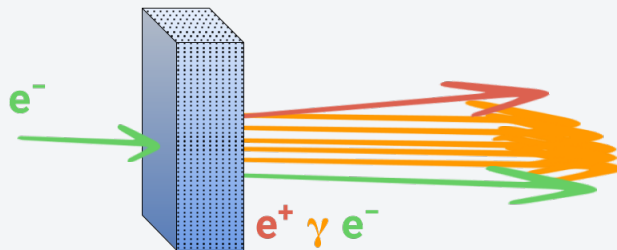


Positron spectrum X. Artru et al. [3]



Coherent effects for crystal-based positron sources

Crystalline photon radiator



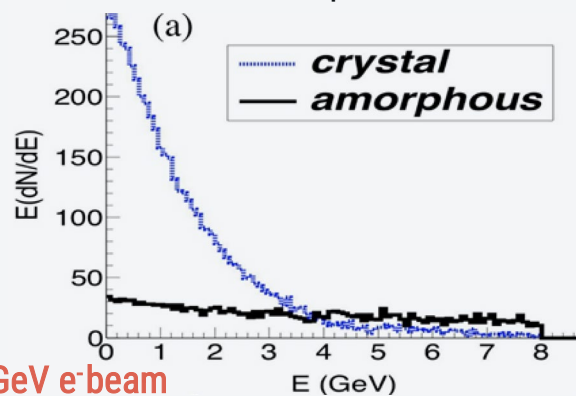
"Thin" oriented crystalline target ($< X_0$)
photon radiator

Hybrid positron source

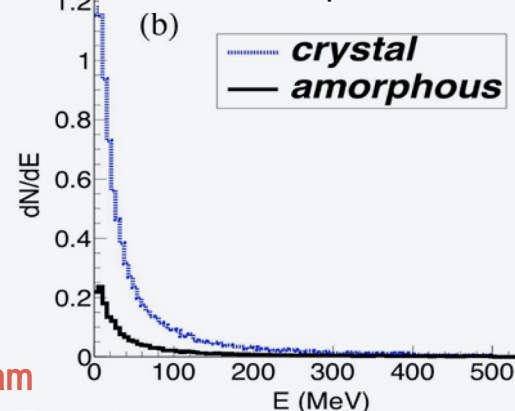


"Thin" crystal ($< X_0$)
photon radiator
Amorphous
target-converter

Photon spectrum *X. Artru et al. [3]*



Positron spectrum *X. Artru et al. [3]*

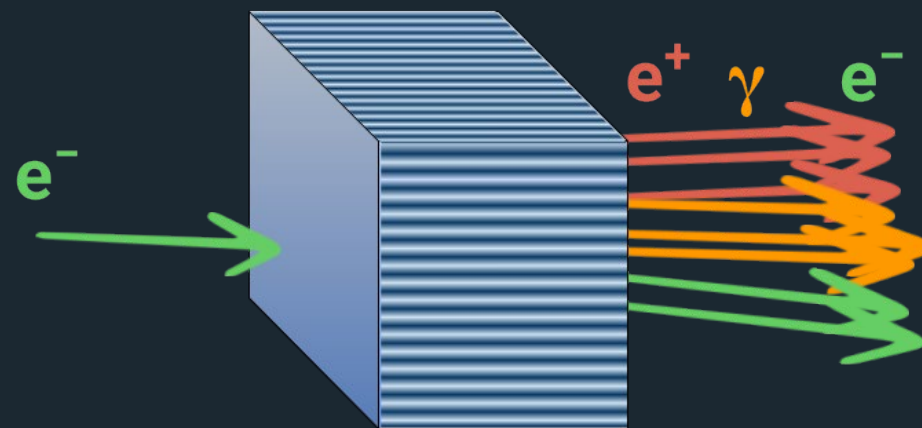


1. Enhancement of photon generation in crystals in coherent conditions → enhancement of pair production in the converter target
2. High rate of soft photons → creation of soft e⁺ easily captured in matching systems
3. Decrease of the PEDD in the converter

Bandiera et al. [4]

Coherent effects for crystal-based positron sources

Or a Single Thick Crystal



The performances are very similar to the hybrid source.

We can use just one device to optimize the positron source of FCC-ee

As seen
in G.Paternò talk

enhancement of
positron generation in
crystals in coherent
conditions \rightarrow
enhancement of pair
production in the
converter target

increase of the PEDD
the converter

Bandiera et al. [4]

Cryst

e^-

"Thin"

250
200
150
100
50
0

8 GeV e^-e^+